

Supplementary Information

Introducing the Substituted AzoBispyrrole Framework: Synthesis and Properties

Adil Alkaş,^a Roberto M. Diaz-Rodriguez,^a Steve O. Sequeira,^a James W. Hilborn,^a Mmasinachi Atansi,^a Em C. Sullivan,^a Emily B. Brown,^a Rosinah Liandrah Gapare,^a Bulent Mutus,^{a,c} Katherine N. Robertson^b and Alison Thompson^{a*}

^aDepartment of Chemistry, PO Box 15000, Dalhousie University, Halifax, Nova Scotia, B3H 4J3, Canada.

^bDepartment of Chemistry, Saint Mary's University, Halifax, NS, B3H 3C3, Canada

^cDepartment of Chemistry & Biochemistry, University of Windsor, 401 Sunset Ave., Windsor N9B3P4, Ontario, Canada

Email: alison.thompson@dal.ca

Contents

Experimental Section	2
General Remarks	2
Synthesis	3
Photophysical Data	5
NMR Spectra	32
X-ray Crystallography	44
References	57

Experimental Section

General Remarks

Reagents and solvents were commercially available, unless stated otherwise, and were used without further purification. Anhydrous solvents were purchased and used without further drying. Nuclear magnetic resonance (NMR) spectra were recorded using either a 500 or a 400 MHz spectrometer. ^1H chemical shifts are reported in ppm relative to tetramethylsilane, referenced to the resonances of CDCl_3 ($\delta = 7.26$ ppm), or d_6 -DMSO ($\delta = 2.50$ ppm) as internal standards. ^{13}C chemical shifts are proton decoupled and reported in ppm relative to tetramethylsilane, referenced to the resonances of CDCl_3 ($\delta = 77.06$ ppm) or d_6 -DMSO ($\delta = 39.53$ ppm). Trace impurities and residual solvent peaks were determined using published tables.¹ Coupling constants are reported in hertz (Hz), and spin multiplicities are reported using the following symbols: s (singlet), bs (broad singlet), d (doublet), t (triplet) and m (multiplet). ^{11}B chemical shifts are reported in ppm, externally referenced to boron trifluoride diethyl etherate ($\delta = 0.00$ ppm). ^{19}F chemical shifts are reported in ppm, externally referenced to CFCl_3 ($\delta = 0.00$ ppm). ^{15}N chemical shifts are reported in ppm, externally referenced to liquid NH_3 ($\delta = 0$ ppm). Thin-layer chromatography was performed using commercially prepared silica gel plates and visualized using long- or short-wave UV lamps. Column chromatography was performed using 40-63 micron particle size (60 Å) silica gel. The relative proportions of solvents mentioned in reference to TLC and column chromatography procedures correspond to volume-to-volume ratios. Mass spectra were recorded using an ion trap instrument operating in electrospray (ESI) mode. Absorption and emission data were recorded in solution at room temperature (RT) using a Horiba Scientific Duetta spectrometer and a quartz cuvette with a 1 cm path length. Molar absorptivity values were recorded at the maximum absorbance in acetonitrile and/or dimethyl formamide. Fluorescence spectra were acquired upon exciting at the absorption maximum and/or as stated. Microwave-promoted experiments were conducted as described in the reaction conditions outlined for relevant compounds. The photodecomposition experiments were performed using either a green LED light (λ_{max} : 520 – 530 nm, Power: 14.4 W), a blue LED light (λ_{max} : 470 – 480 nm, Power: 14.4 W) or a UV LED light (λ_{max} : 390 – 400 nm, Power: 14.4 W) within a plastic 3D printed ring and using a stir plate, all as stated. Solid state emission data were recorded using a Wilson Analytical Open Platform System (OPS) equipped with an Ocean Insight Flame spectrometer (range 190-1100 nm) using LED excitation light sources with either UV (λ_{max} : 365 nm, Power 800 mW) or green light (λ_{max} : 550 nm, Power: 1500 mW). Absorption and emission spectra in solutions were recorded using a Horiba Duetta spectrometer and a quartz cuvette.

Synthesis

Chalcone **1** and nitrobutanone **2** were synthesized according to literature procedures.²

2, 2'-Diazenediylbis(3-(2,4,6-trimethylphenyl)-5-phenyl-1*H*-pyrrole) (**3**)

To a 30 mL microwave vial was added a magnetic stirrer bar, nitrobutanone **2** (0.5 g, 1.6 mmol), ammonium acetate (5.2 g, 68 mmol) and glacial acetic acid (15 mL). The vial was sealed and warmed to ~60°C, by use of a hot plate, to dissolve the solids. The material was allowed to cool to near room temperature and then placed in the microwave reactor and irradiated (20 minutes, 118°C, 80 W, 780 RPM, Very High Absorbance). This reaction was run in duplicate and the mixtures subsequently combined before adding to CH₂Cl₂ (100 mL). The organic layer was washed with water (2 x 200 mL) and brine (200 mL). The organic layer was then dried (Na₂SO₄), filtered and concentrated. The crude mixture was purified by column chromatography over silica (0 → 20% EtOAc:hexanes). In vacuo evaporation of the fractions containing the desired product resulted in a red solid. This solid was dissolved a minimum amount of dichloromethane. Cold pentane (100 mL) was added, and the solution was cooled for 2 hours, in a freezer. The resultant precipitate was isolated via filtration and washed with cold pentane (2 x 25 mL) to provide **3** as a bright red solid (0.26 g, 30%). UV-Vis: λ_{max} (MeCN) 504 (ε 6.3 x 10⁴), 522 (6.3 x 10⁴); (DMF) 504 (ε 5.1 x 10⁴), 532 (5.4 x 10⁴). ¹H NMR (d₆-DMSO, 500 MHz): δ 11.41 (bs, 2H), 7.80 (d, *J* = 7.5 Hz, 4H), 7.37 (t, *J* = 8.3 Hz, 4H), 7.22 (t, *J* = 7.5 Hz, 2H), 6.70 (s, 4H), 6.53 (s, 2H), 2.29 (s, 6H), 1.82 (s, 12H). ¹³C{¹H} NMR (125 MHz, d₆-DMSO): δ 144.3, 137.0, 135.3, 133.5, 132.3, 132.0, 129.2, 127.7, 127.2, 124.9, 122.6, 110.7, 21.3, 21.0. ¹H-¹⁵N HMBC NMR (CDCl₃, 500 MHz): δ (6.51, 125.3), (6.51, 525.6). HRMS (ESI-TOF) (m/z): [M + Na]⁺ Calcd for C₃₈H₃₆N₄Na 571.2832; Found 571.2834.

Concentration of the earlier-running column chromatographic fractions provided a residue containing the aza-dipyrin **4**. This residue was purified by column chromatography on silica eluting with CH₂Cl₂ to provide the aza-dipyrin N-(5-phenyl-3-(2,4,6-trimethylphenyl)-2H-pyrrole-2-ylidene)-5-phenyl-3-(2,4,6-trimethylphenyl)-1H-pyrrole-2-amine (**4**, previously reported² without full characterization data) as a purple solid: (0.15 g, 18%). UV-Vis: λ_{max} (MeCN) 288 (ε 4.5 x 10⁴), 570 (4.0 x 10⁴). ¹H NMR (CDCl₃, 500 MHz): δ 7.93 (d, *J* = 7.2 Hz, 4H), 7.53 (t, *J* = 7.6 Hz, 4H), 7.45 (t, *J* = 7.3 Hz, 2H), 6.81 (s, 4H), 6.79 (s, 2H), 2.27 (s, 6H), 2.10 (s, 12H). ¹³C{¹H} NMR (CDCl₃, 100 MHz): δ 154.9, 149.9, 144.4, 136.8, 136.6, 132.3, 131.0, 129.9, 129.1, 127.7, 126.5, 118.8, 21.1, 20.9. ¹H-¹⁵N HMBC NMR (CDCl₃, 500 MHz): δ (6.81, 203.1), (6.81, 603.7). HRMS (ESI-TOF) m/z: [M + H]⁺ Calcd for C₃₈H₃₆N₃ 534.2904; Found 534.2916.

N,N-Dimethylated azobispyrrole (**5a**) and *N*-methylated azobispyrrole (**5b**)

Following a modified literature procedure,³ to a 50 mL round-bottom flask was added azo bispyrrole **3** (20 mg, 0.037 mmol) and K₂CO₃ (88 mg, 0.66 mmol). Anhydrous MeCN (25 mL) was added, followed by iodomethane (0.2 mL, 3.2 mmol). The mixture was heated at 60°C for 1.5 hours and the reaction monitored for completion using TLC (5% EtOAc:hexanes). The contents were then allowed to cool to room temperature, and then concentrated in vacuo. The residue was dissolved in EtOAc (50 mL) and washed with 0.01 aq. M HCl (25 mL) and brine (25 mL). The organic layer was then dried (Na₂SO₄), filtered and concentrated in vacuo to yield an oil. The oil was purified using column chromatography over silica (3% EtOAc:hexanes). Subsequent purification using column chromatography over silica (10% CH₂Cl₂:hexanes) provided *N,N*-dimethylated azobispyrrole **5a** and *N*-methylated azobispyrrole **5b**. Crystals of **5a** were obtained via slow growth from a solution in pentane and provided a shiny red solid: (8 mg, 39%). The monomethyl product **5b** was isolated as an oil: (4 mg, 19%).

N,N-Dimethylated azobispyrrole (5a)

UV-Vis: λ_{\max} (MeCN) 510 (ϵ 2.8 x 10⁴); (DMF) 514 (ϵ 2.8 x 10⁴). ¹H NMR (400 MHz, CDCl₃) δ : 7.63-7.35 (m, 8H), 7.34-7.27 (m, 2H), 6.87 (s, 4H), 6.10 (s, 2H), 3.12 (s, 6 H), 2.28 (s, 6H), 2.04 (s, 12H). ¹³C{¹H} NMR (CDCl₃, 100 MHz,) δ : 143.6, 136.7, 136.0, 135.2, 134.5, 132.7, 128.5, 128.3, 127.5, 127.1, 112.7, 111.8, 30.6, 21.0, 20.8. HRMS (ESI-TOF) m/z: [M + Na]⁺ Calcd for C₄₀H₄₀N₄Na 599.3145; Found 599.3153.

N-Methylated azobispyrrole (5b)

UV-Vis: λ_{\max} (MeCN) 512 (ϵ 3.7 x 10⁴); (DMF) 518 (ϵ 3.7 x 10⁴). ¹H NMR (CDCl₃, 400 MHz): δ 9.17 (bs, 1H), 7.57-7.32 (m, 10H), 6.86 (s, 2H), 6.63 (s, 2H), 6.45 (s, 1H), 6.17 (s, 1H), 3.88 (s, 6 H), 2.40 (s, 3H), 2.31 (s, 3H), 1.96 (s, 12H). ¹³C{¹H} NMR (CDCl₃,100 MHz,) δ : 143.6, 142.9, 136.4, 137.1, 137.1, 135.8, 135.4, 132.7, 132.5, 132.5, 131.6, 131.1, 130.9, 129.0, 128.6, 128.6, 127.5, 127.4, 127.3, 127.2, 124.1, 112.7, 110.3, 32.9, 21.2, 20.7 (2 signals missing). HRMS (ESI-TOF) m/z: [M + H]⁺ Calcd for C₃₉H₃₉N₄ 563.3169; Found 563.3175.

BF₂ Adduct (6)

To a solution of azo bispyrrole **3** (43 mg, 0.08 mmol) in anhydrous CH₂Cl₂ (10 mL) was added triethylamine (0.5 mL, 3.61 mmol) at RT under nitrogen, and the mixture was stirred for 10 minutes. Boron trifluoride diethyl etherate (1.00 mL, 8.11 mmol) was then added, and the mixture stirred for 2 hours. After removal of the solvent under reduced pressure, the crude material was dissolved in pentane (20 mL) and washed with water (20 mL) and brine (20 mL). The organic layer was dried (Na₂SO₄), filtered and concentrated in vacuo. The residue was purified using column chromatography over silica (0 → 30% CH₂Cl₂:hexanes) to provide **6** as a blue solid: (33 mg, 70% yield). UV-Vis: λ_{\max} (MeCN) 666 (ϵ 4.7 x 10⁴); (DMF) 672 (ϵ 4.8 x 10⁴). ¹H NMR (CDCl₃, 500 MHz): δ 9.19 (d, *J* = 3.1 Hz, 1H), 7.79-7.77 (m, 2H), 7.58-7.56 (m, 2H), 7.43-7.30 (m, 6H), 6.98 (s, 2H), 6.91 (s, 2H), 6.65 (s, 1H), 6.47 (d, *J* = 3.1 Hz, 1H), 2.38 (s, 3H), 2.35 (s, 3H), 2.20 (s, 6H), 2.14 (s, 6H). ¹³C{¹H} NMR (CDCl₃, 125 MHz): δ 148.0, 138.2, 137.8, 137.3, 137.2, 134.5, 133.2, 130.5, 130.4, 129.9, 129.2, 129.1, 128.9, 128.3, 128.0, 127.4, 127.1, 124.5, 122.9, 118.8, 112.3, 21.2, 21.1, 20.8 ppm. ¹¹B NMR (CDCl₃, ¹160 MHz): δ 3.5 (s). ¹⁹F NMR (CDCl₃, 470 MHz): δ -154.5 (s), -154.6 (s). HRMS (ESI-TOF) m/z: (M + Na)⁺; Calcd for C₃₈H₃₅BF₂N₄Na 619.2812; Found 619.2815.

Photophysical Data

Figure S1: Normalized absorption and emission spectra of a solution of compound 3 in MeCN

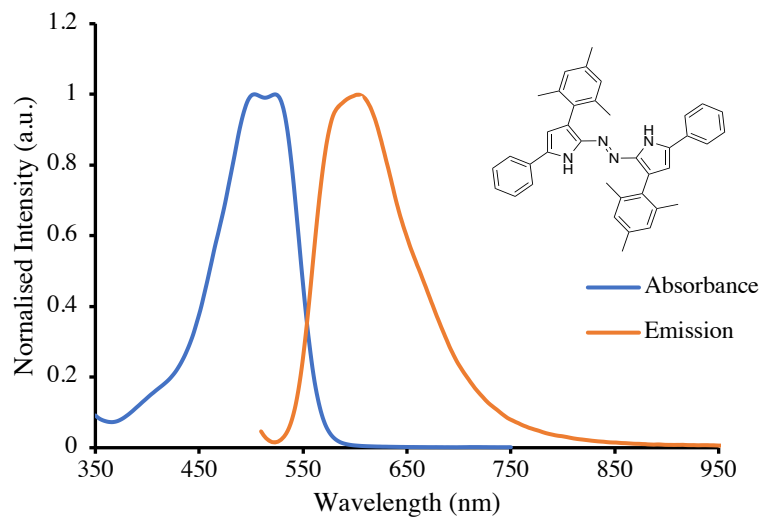


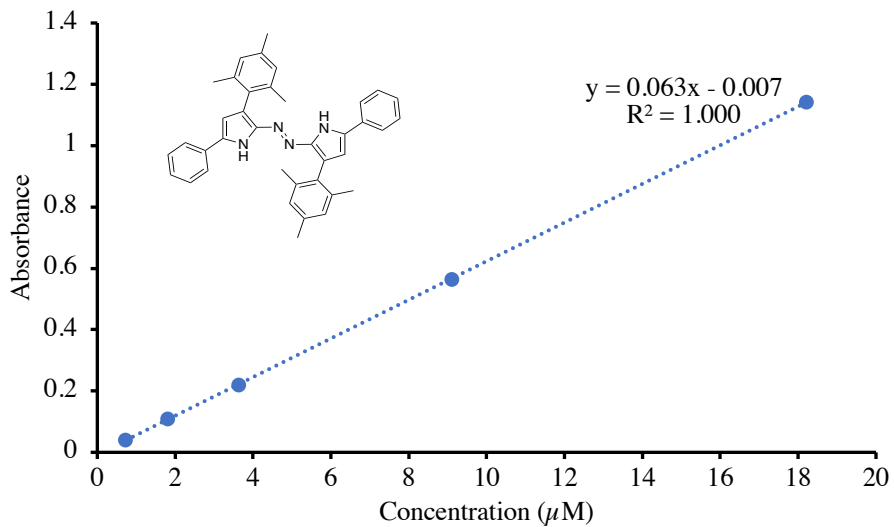
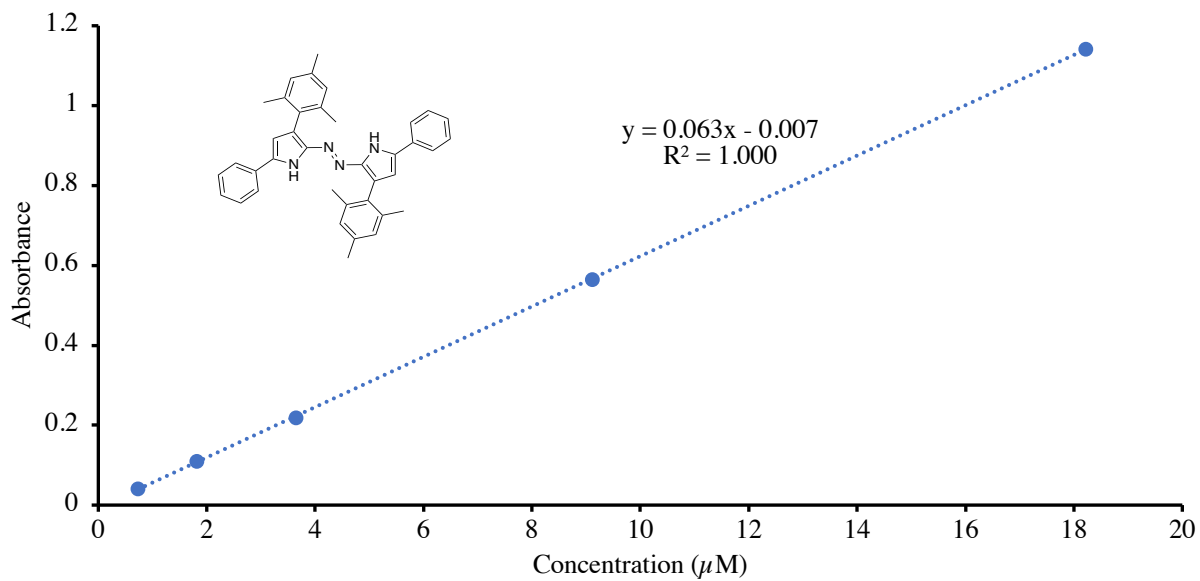
Figure S2: Calibration curve of a solution compound of 3 in MeCN at 504 nm**Figure S3: Calibration curve of a solution of compound 3 in MeCN at 522 nm**

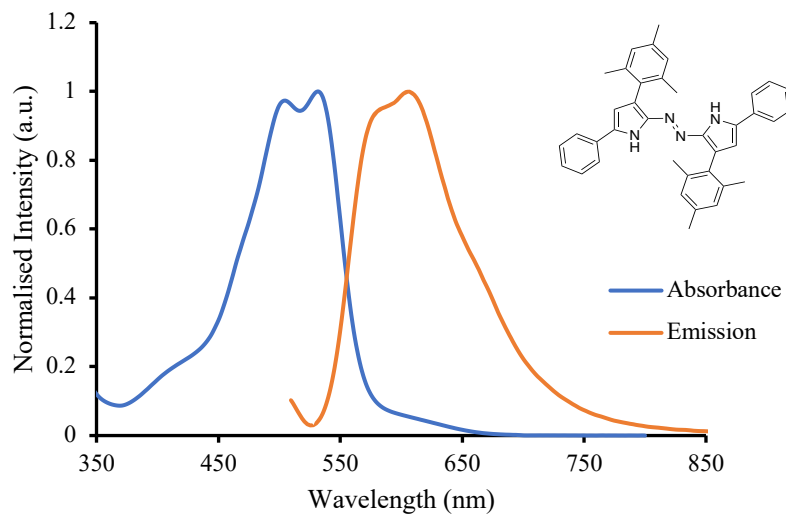
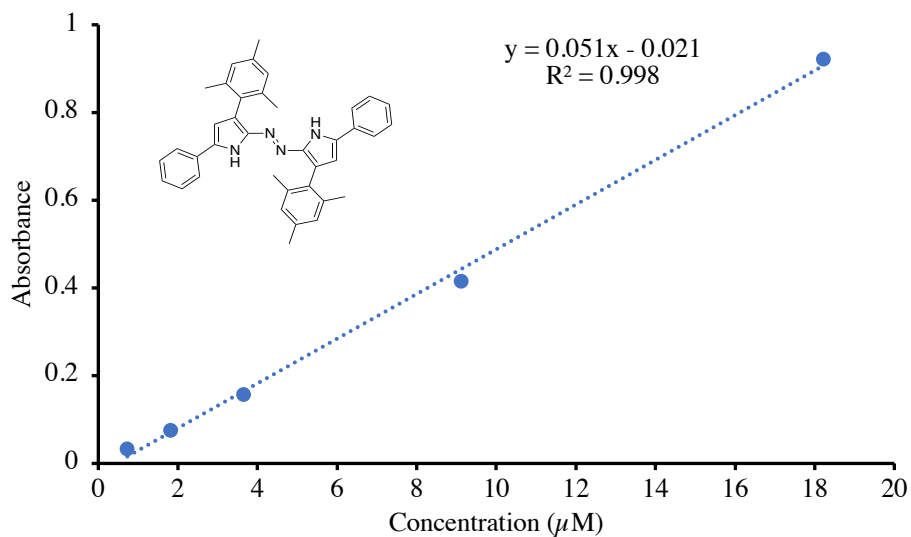
Figure S4: Normalized absorption and emission spectra of a solution of compound 3 in DMF**Figure S5: Calibration curve of a solution of compound 3 in DMF at 504 nm**

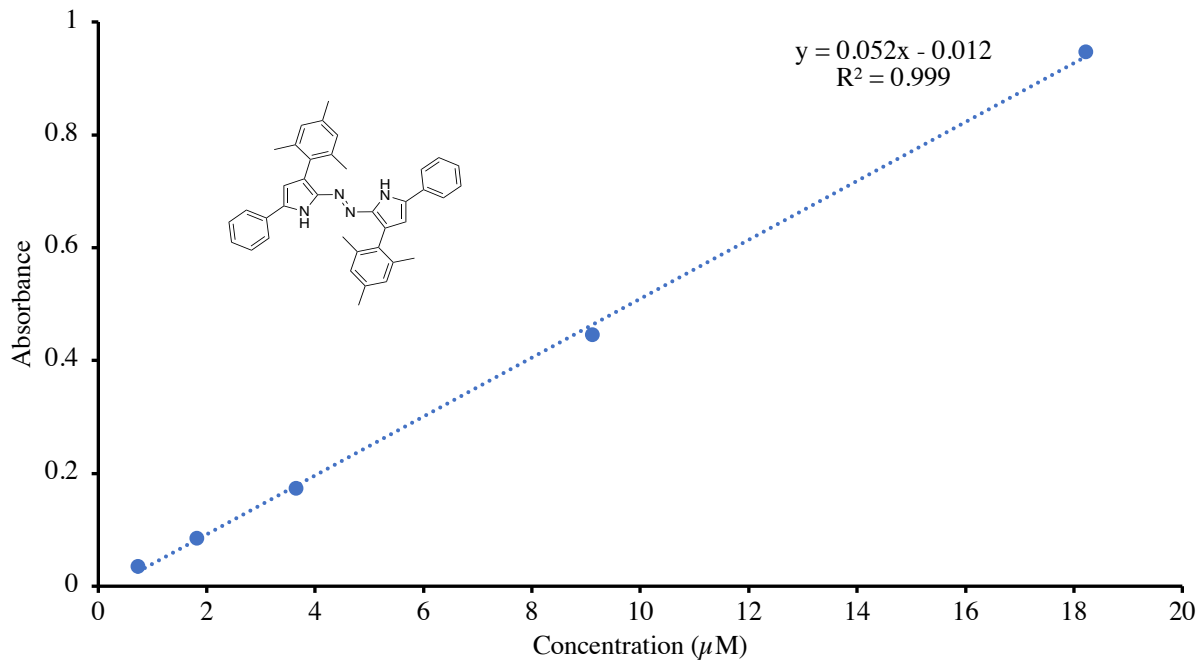
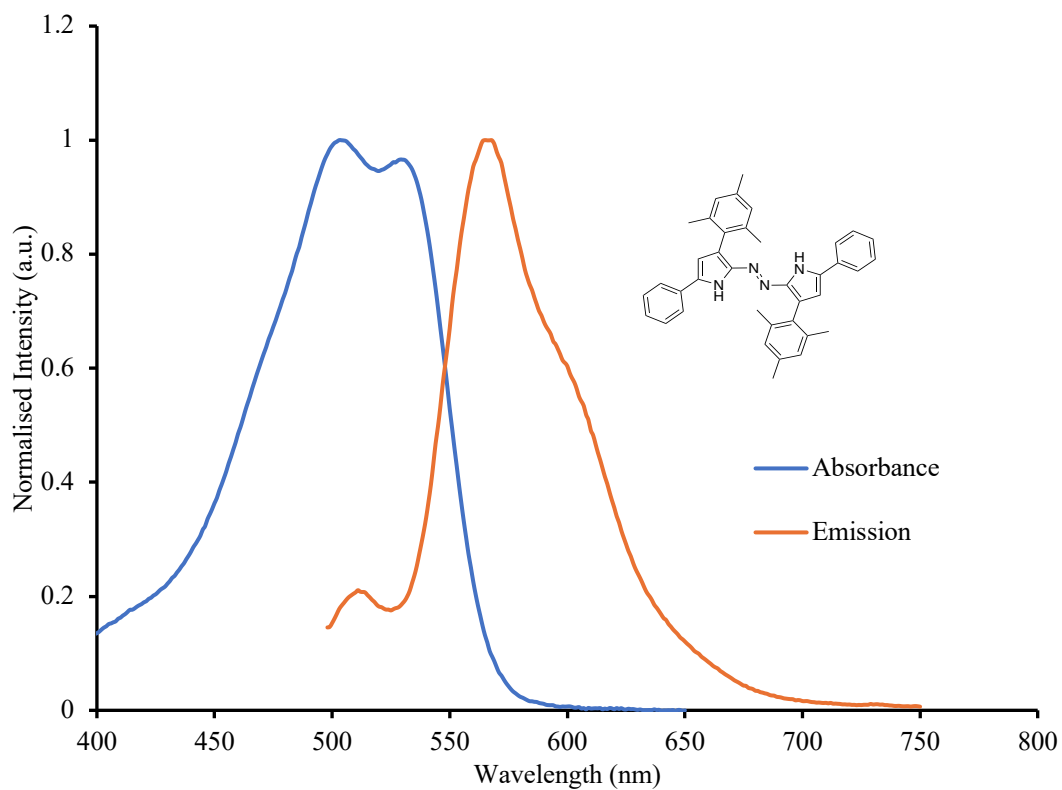
Figure S6: Calibration curve of a solution of compound 3 in DMF at 532 nm**Figure S7: Normalized absorption and emission spectra of a solution of compound 3 in THF**

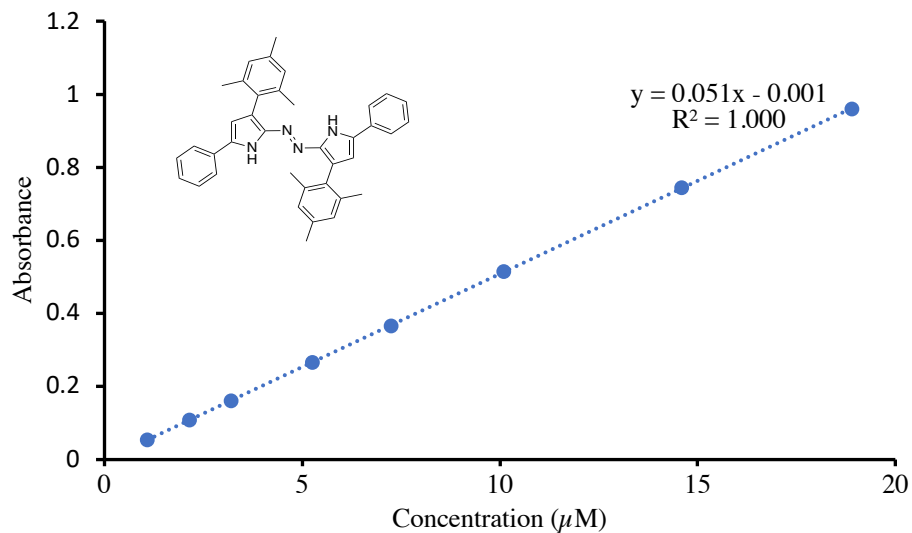
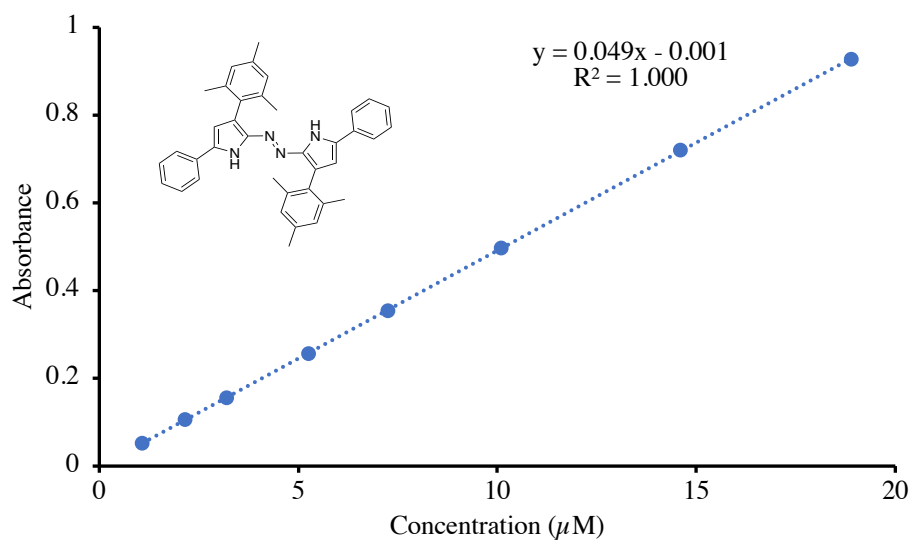
Figure S8: Calibration curve of a solution of compound 3 in THF at 504 nm**Figure S9: Calibration curve of a solution of compound 3 in THF at 529 nm**

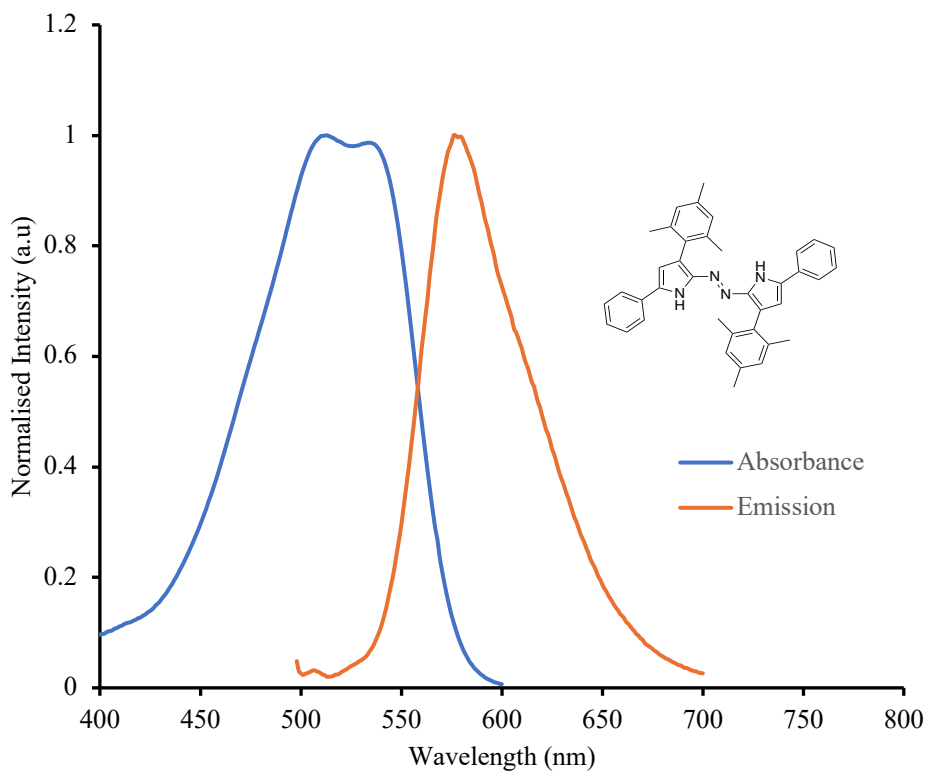
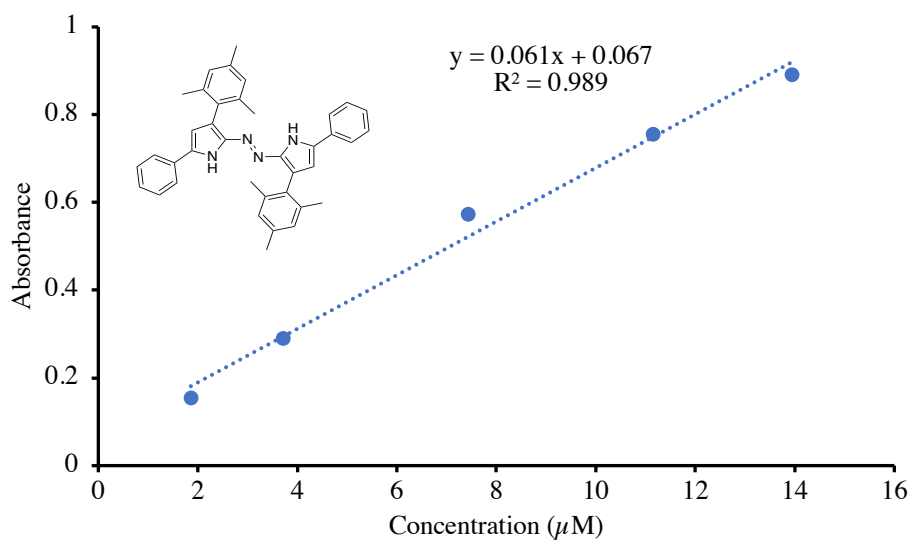
Figure S10: Normalized absorption and emission spectra of a solution of compound 3 in CH₂Cl₂**Figure S11: Calibration curve of a solution of compound 3 in CH₂Cl₂ at 513 nm**

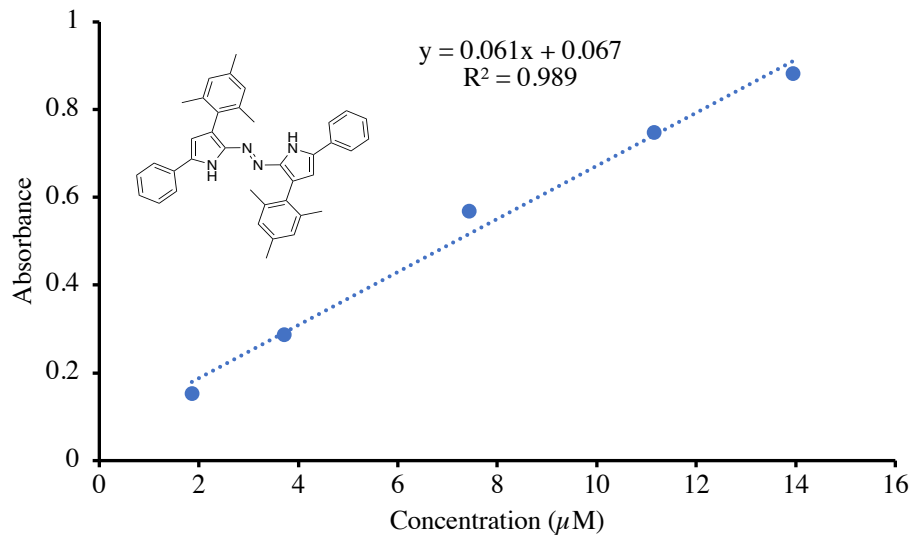
Figure S12: Calibration curve of a solution of compound 3 in CH₂Cl₂ at 529 nm

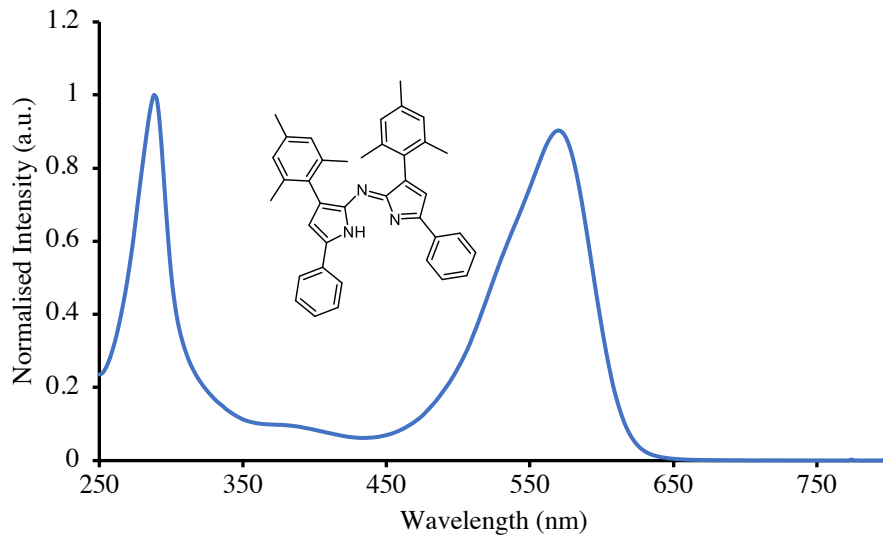
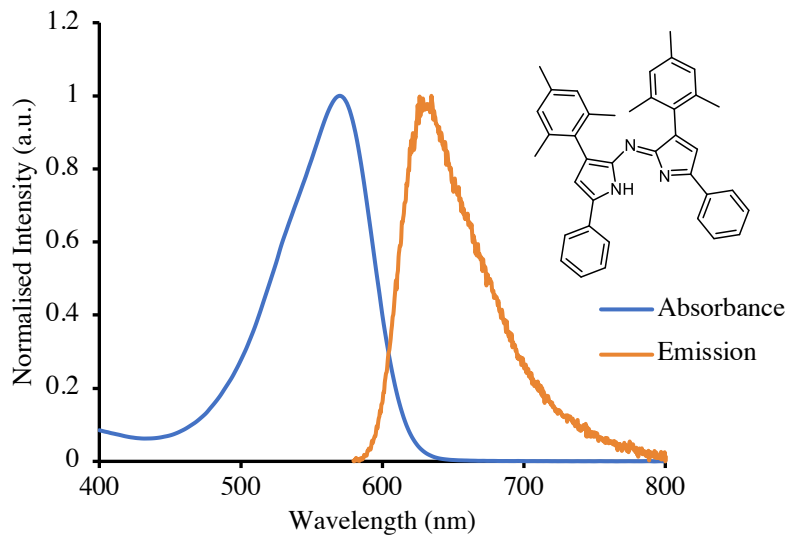
Figure S13: Normalized absorption spectrum of a solution of compound 4 in MeCN**Figure S14: Normalized absorption and emission spectra of a solution of compound 4 in MeCN**

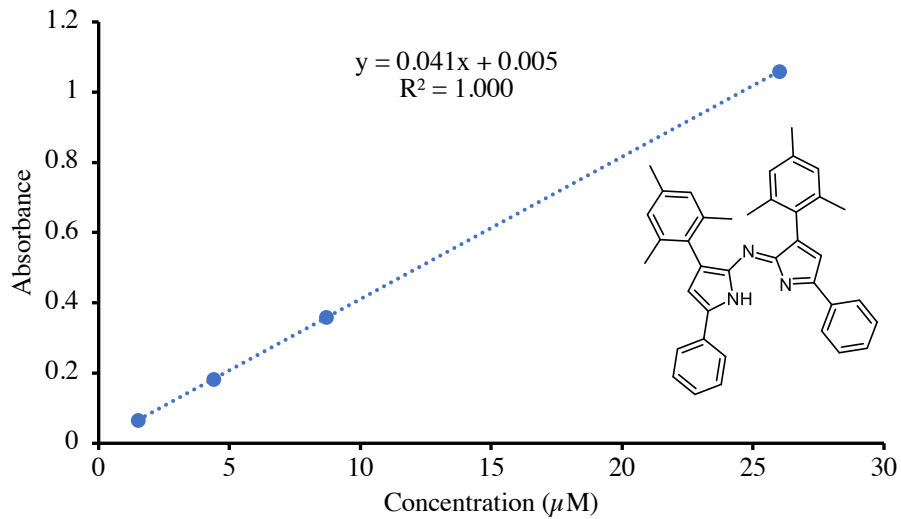
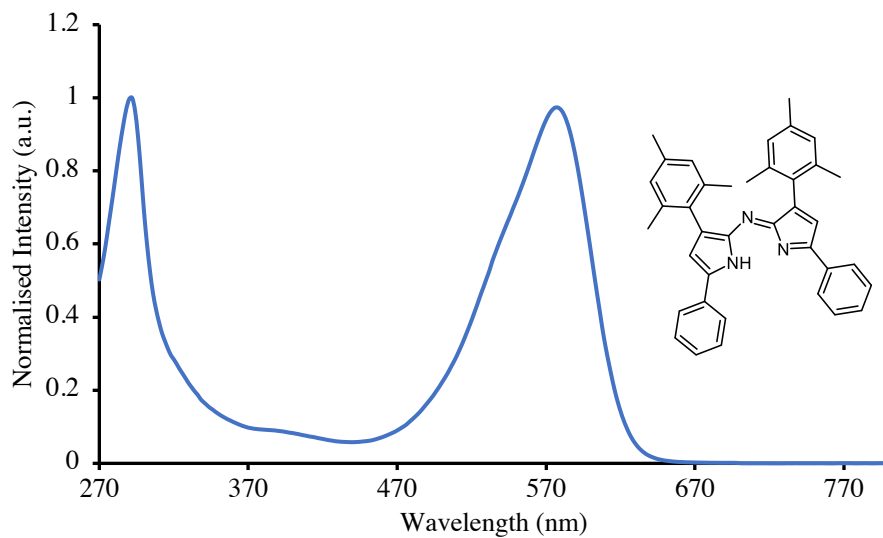
Figure S15: Calibration curve of a solution of compound 4 in MeCN at 570 nm**Figure S16: Normalized absorption spectrum of a solution of compound 4 in DMF**

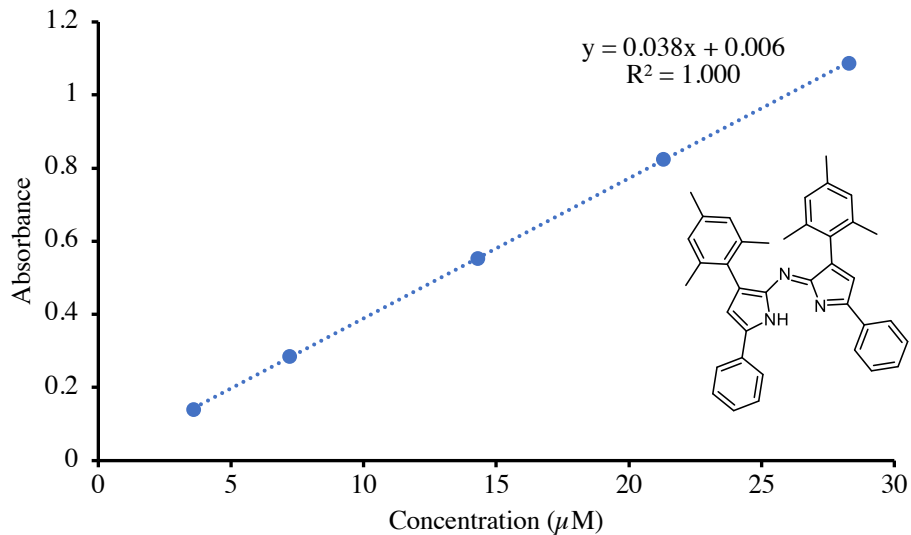
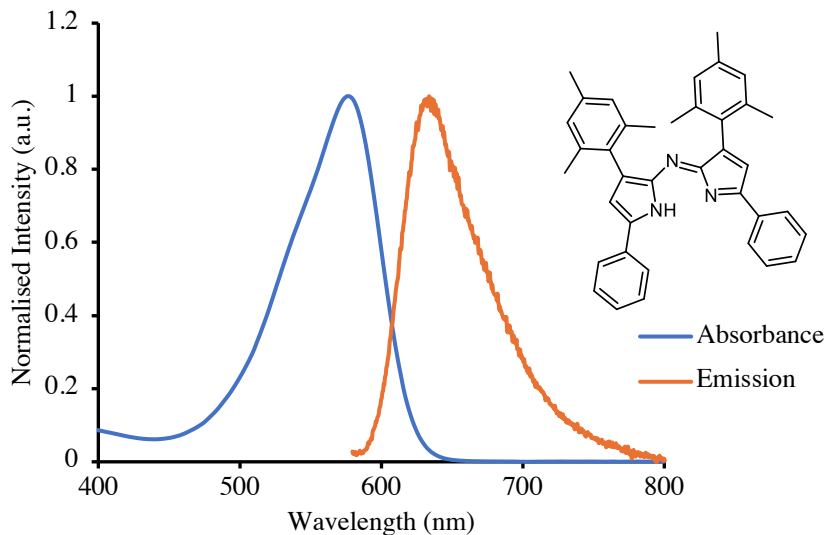
Figure S17: Calibration curve of a solution of compound 4 in DMF at 576 nm**Figure S18: Normalized absorption and emission spectra of a solution of compound 4 in DMF**

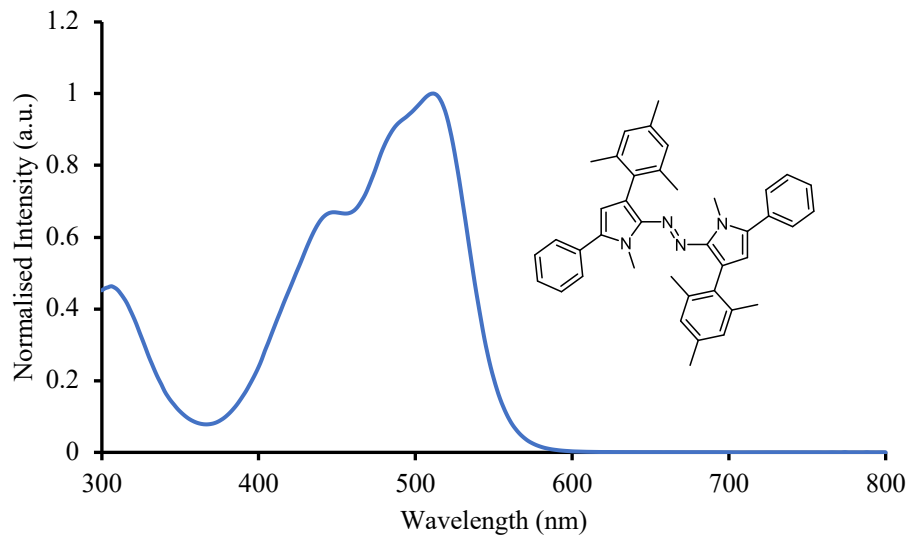
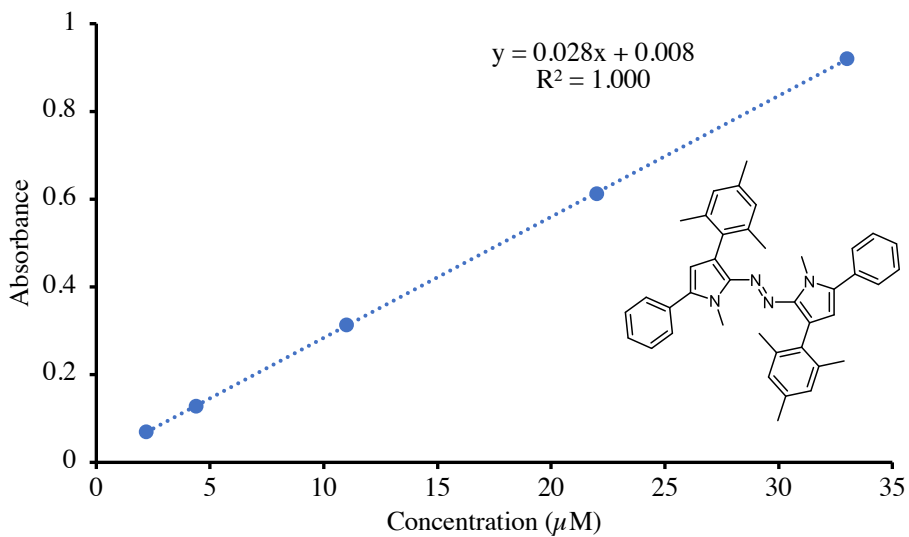
Figure S19: Normalized absorption spectrum of a solution of compound 5a in MeCN**Figure S20: Calibration curve of a solution of compound 5a in MeCN at 510 nm**

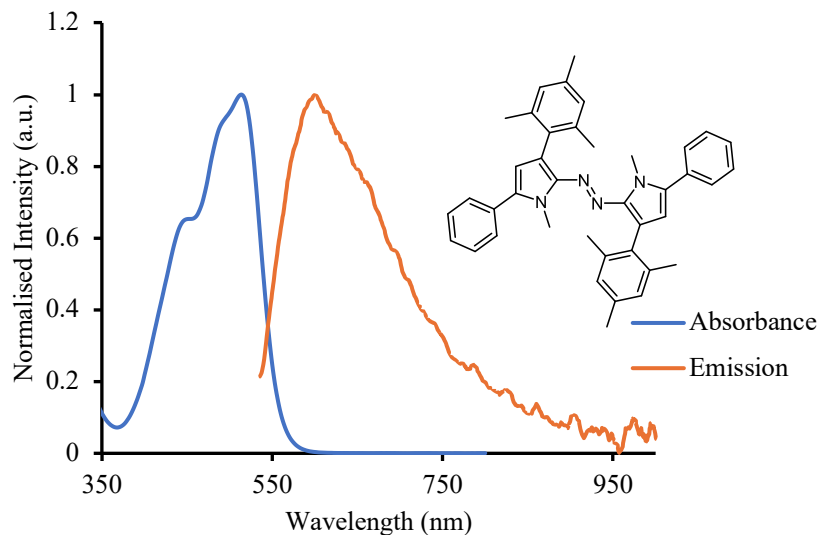
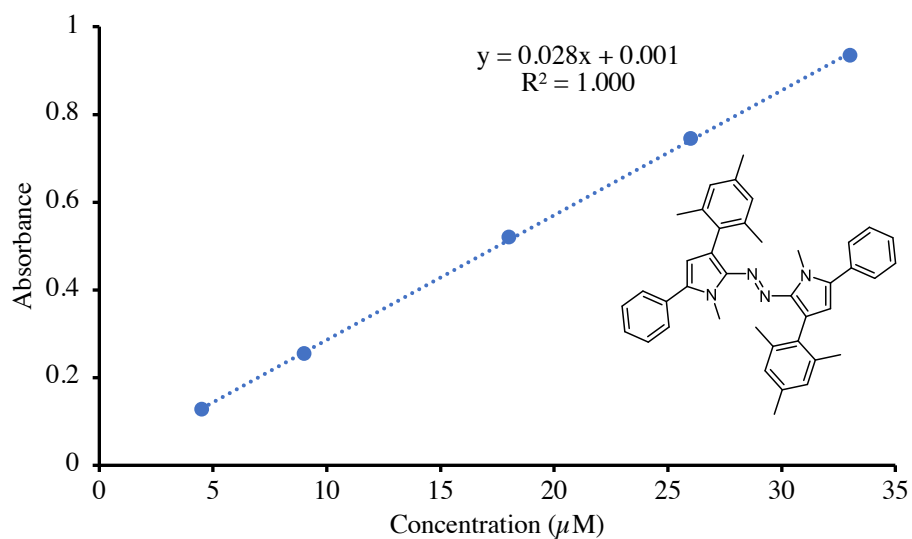
Figure S21: Normalized absorption and emission spectra of a solution of compound 5a in DMF**Figure S22: Calibration curve of a solution of compound 5a in DMF at 514 nm**

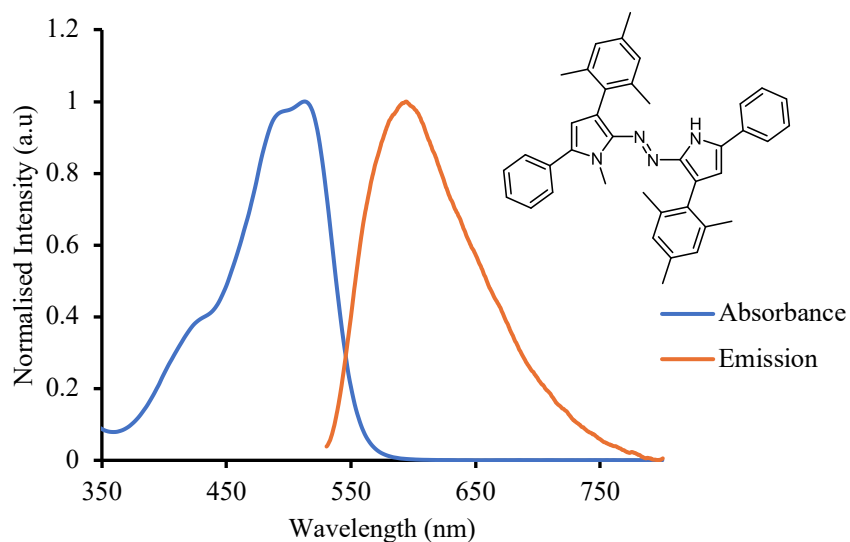
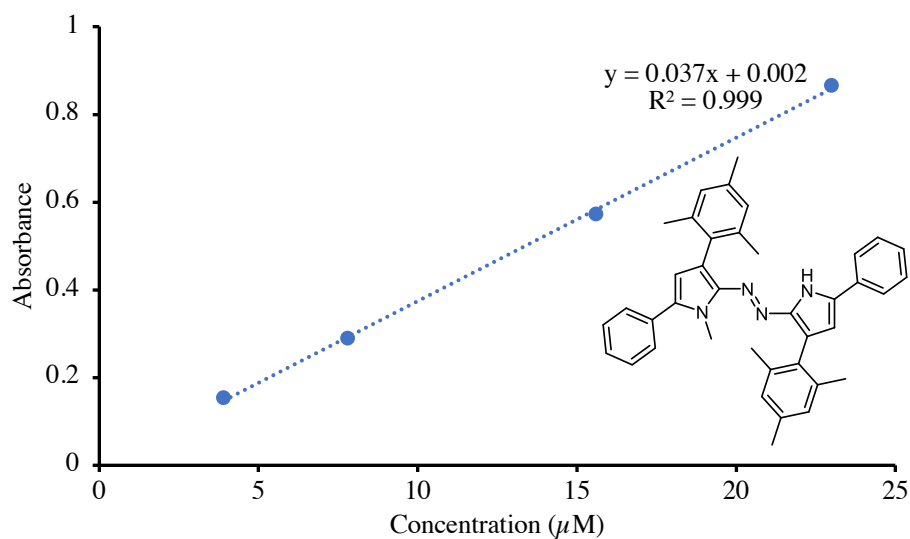
Figure S23: Normalized absorption and emission spectra of a solution of compound 5b in MeCN**Figure S24: Calibration curve of a solution of compound 5b in MeCN at 512 nm**

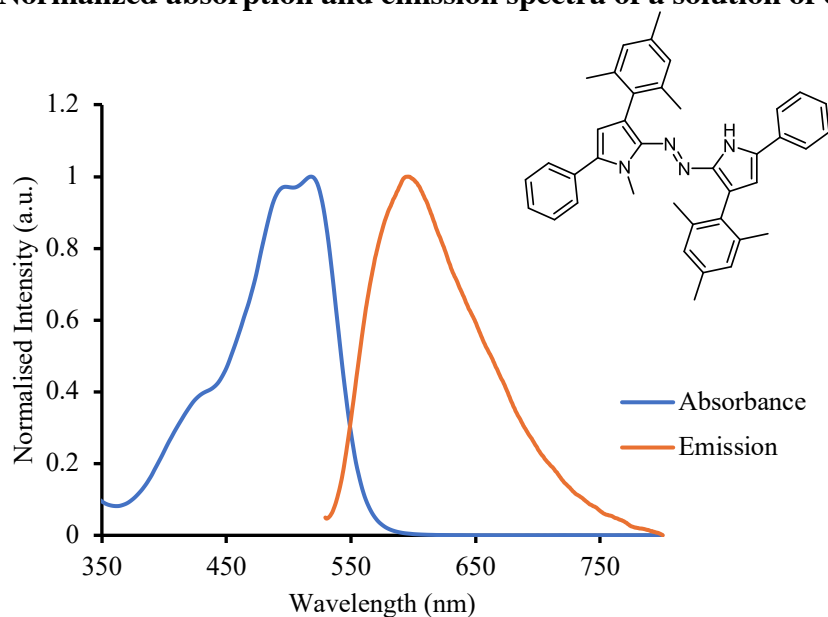
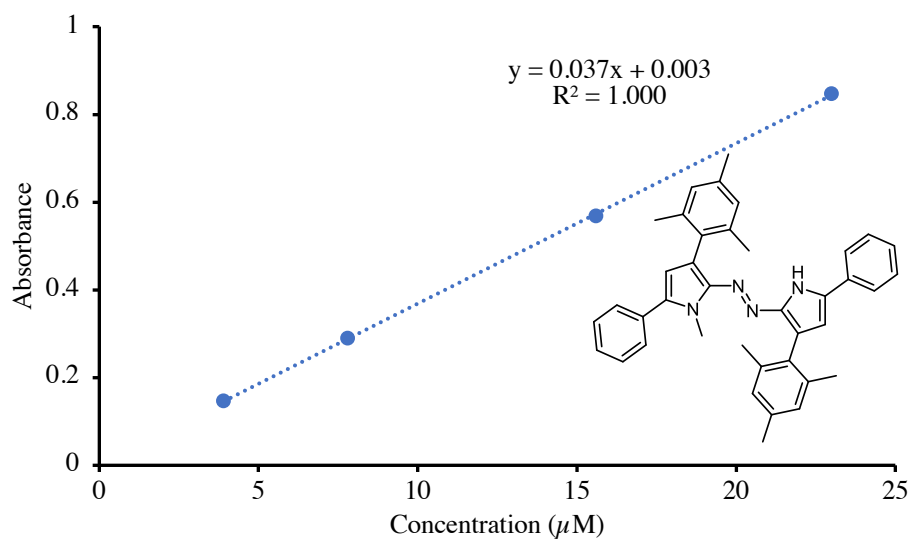
Figure S25: Normalized absorption and emission spectra of a solution of compound 5b in DMF**Figure S26: Calibration curve of a solution of compound 5b in DMF at 518 nm**

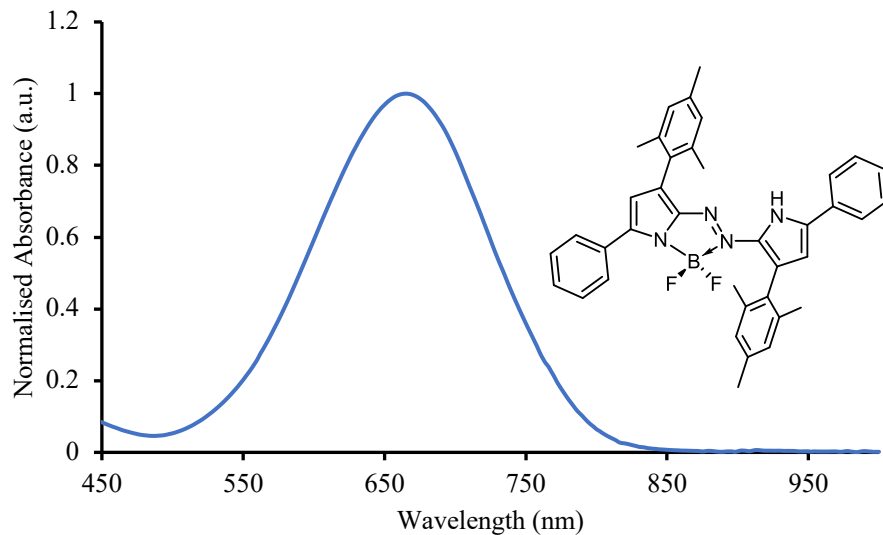
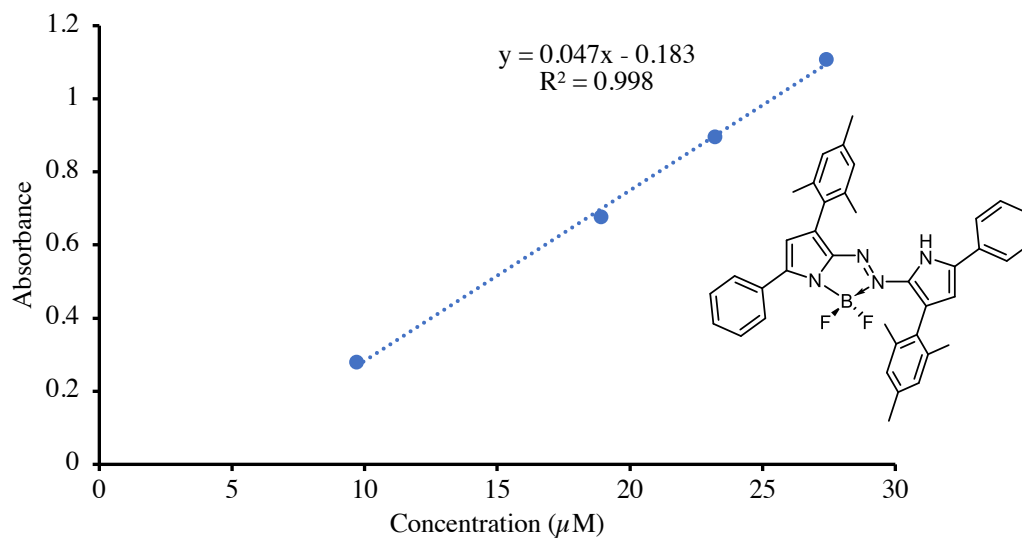
Figure S27: Normalized absorption spectrum of a solution of compound 6 in MeCN**Figure S28: Calibration curve of a solution of compound 6 in MeCN**

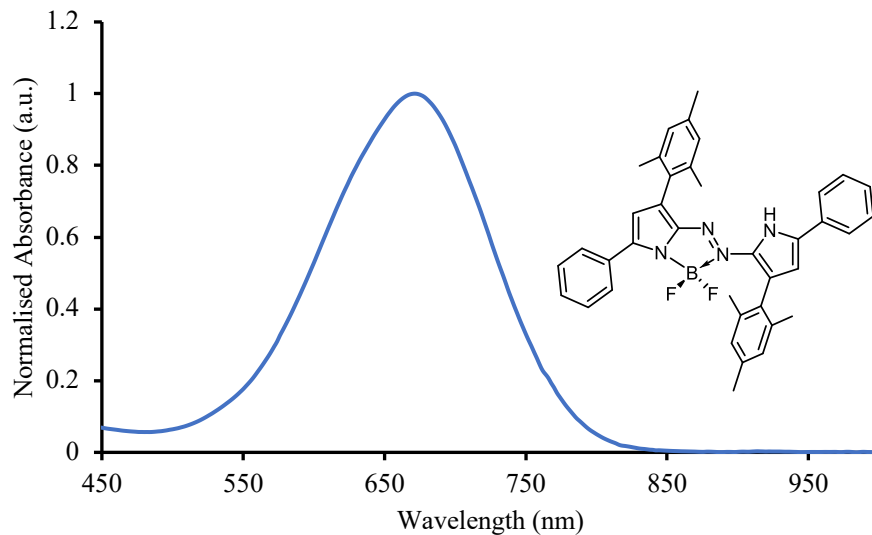
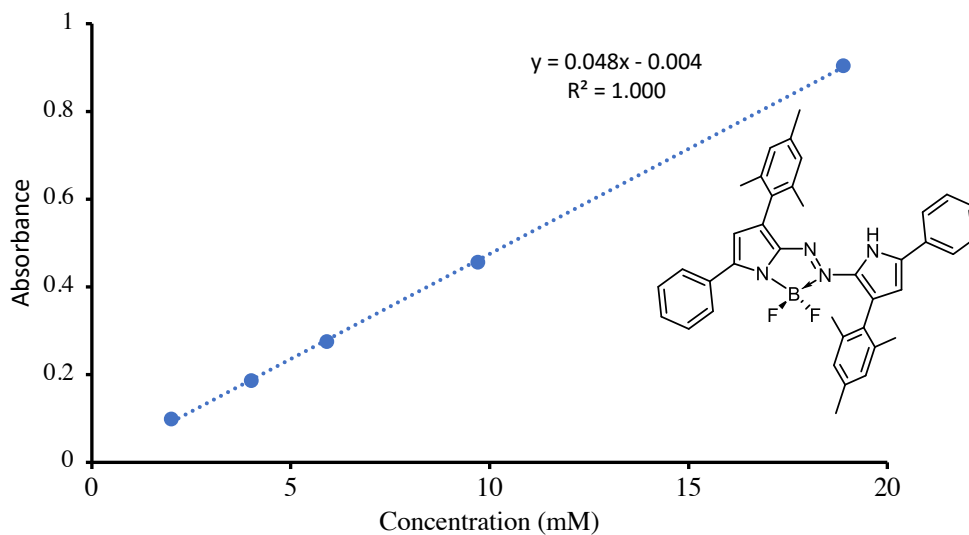
Figure S29: Normalized absorption spectrum of a solution of compound 6 in DMF**Figure S30: Calibration curve of a solution of compound 6 in DMF**

Figure S31: Absorbance spectra of 9×10^{-6} M solutions of compound 3 in CH_2Cl_2 monitored over 72 hours. (left = sample exposed to sunlight, right = sample kept in the dark).

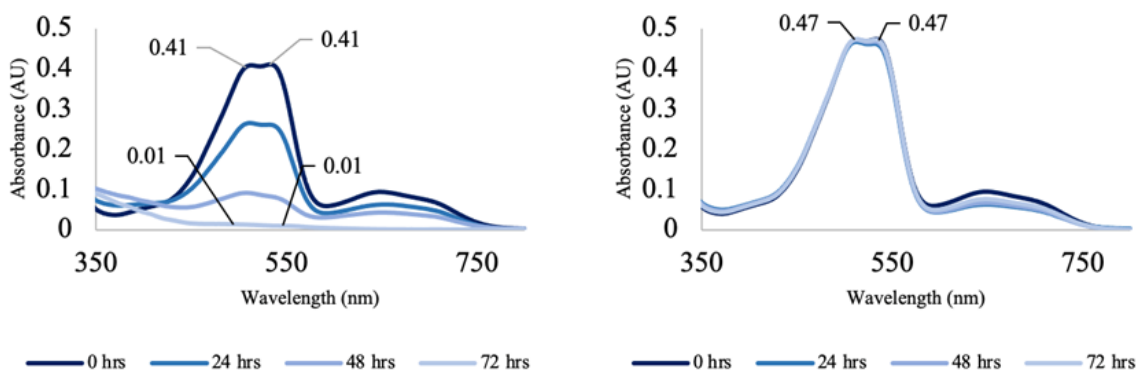


Figure S32: Photo-decay of compound 3 in CH_2Cl_2 over 72 hours.



Figure S33: Absorption spectra of solution of compound 3 in MeCN under a N₂ atmosphere upon exposure to LED light (390 nm) for the indicated period of time.

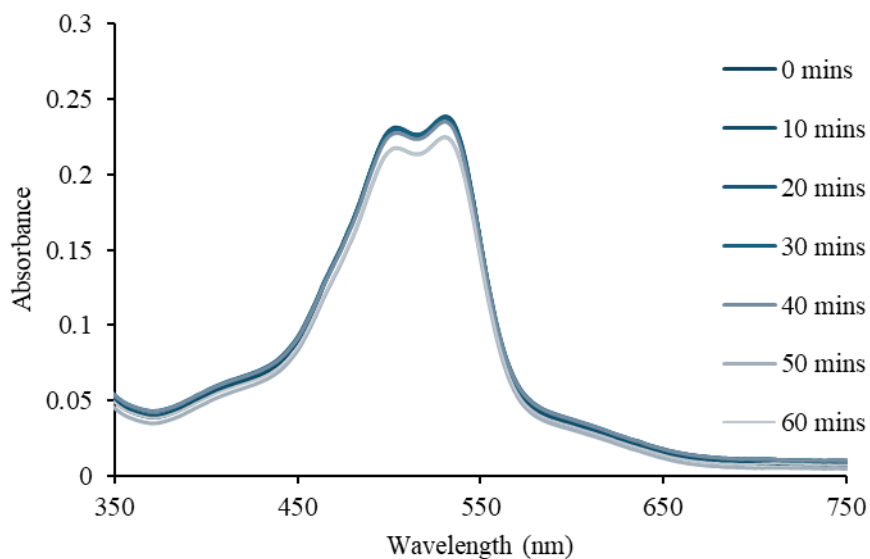


Figure S34: Absorption spectra of solution of compound 3 in MeCN under a N₂ atmosphere upon exposure to LED light (460 nm) for the indicated period of time.

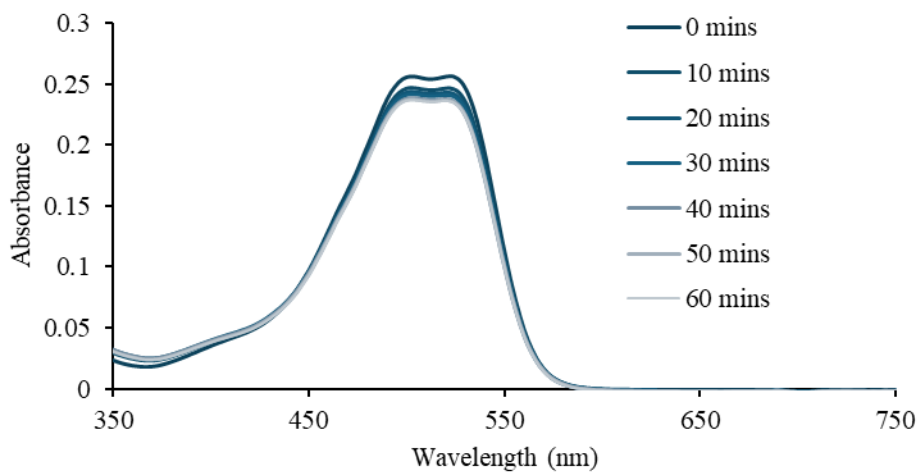


Figure S35: Absorption spectra of solution of compound 3 in MeCN under a N₂ atmosphere upon exposure to LED light (520 nm) for the indicated period of time.

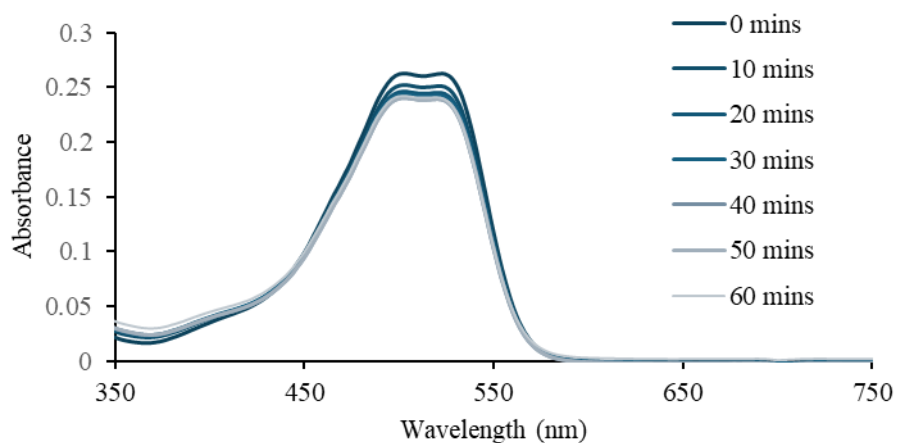


Figure S36: Absorbance spectra of a solution of compound 3 in MeCN upon exposure to LED light (520 nm) for the indicated period of time.

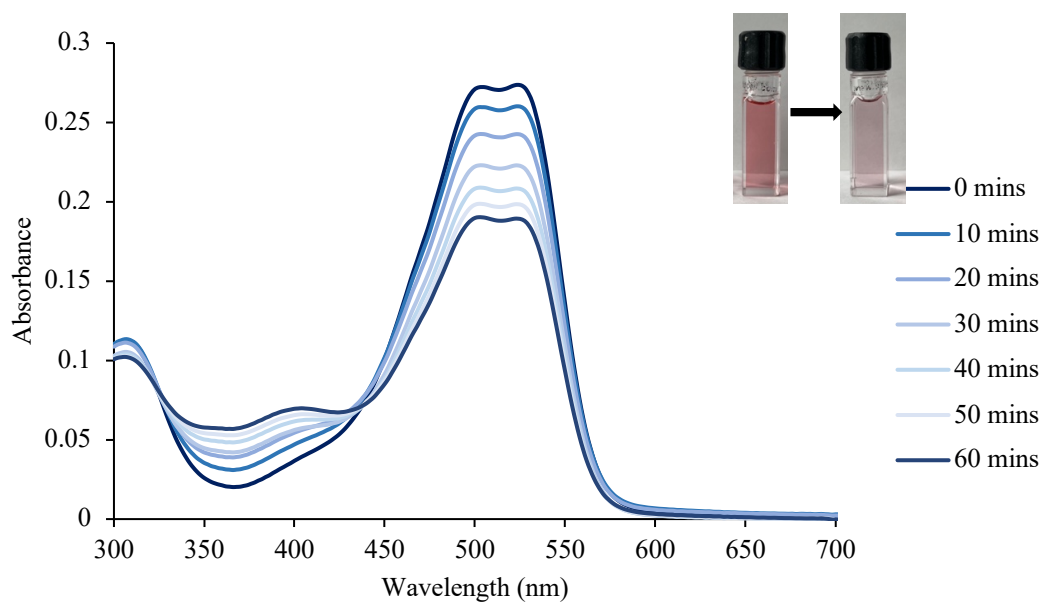


Figure S37: Absorption spectra of solution of compound 3 in DMF under a N₂ atmosphere upon exposure to LED light (390 nm) for the indicated period of time.

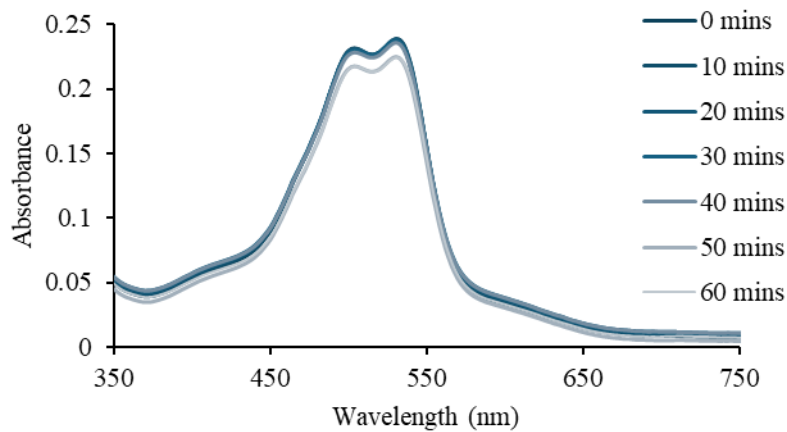


Figure S38: Absorption spectra of solution of compound 3 in DMF under a N₂ atmosphere upon exposure to LED light (460 nm) for the indicated period of time.

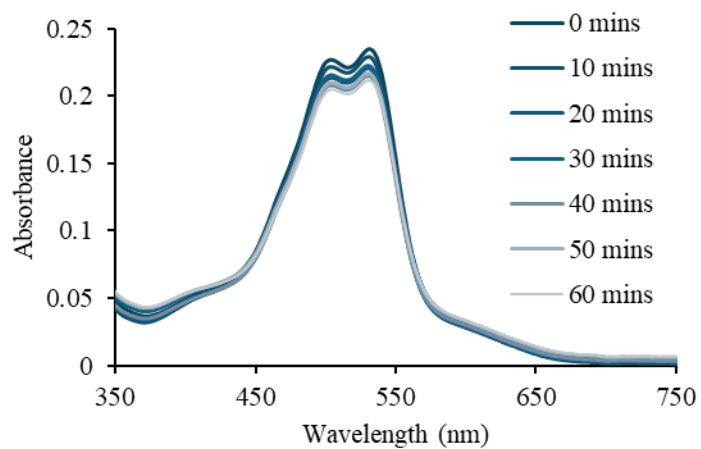


Figure S39: Absorption spectra of solution of compound 3 in DMF under a N₂ atmosphere upon exposure to LED light (520 nm) for the indicated period of time.

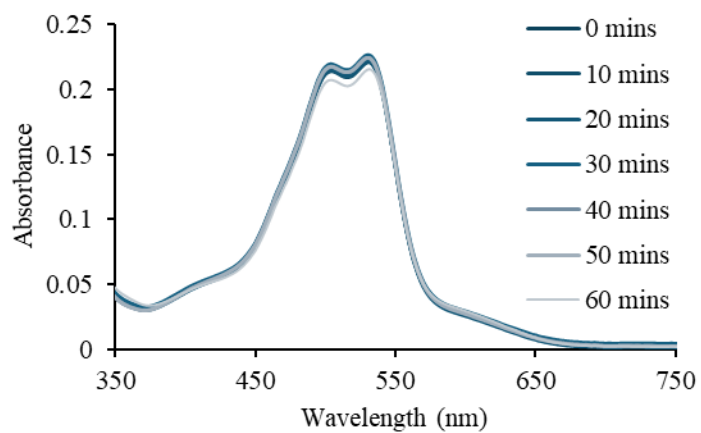


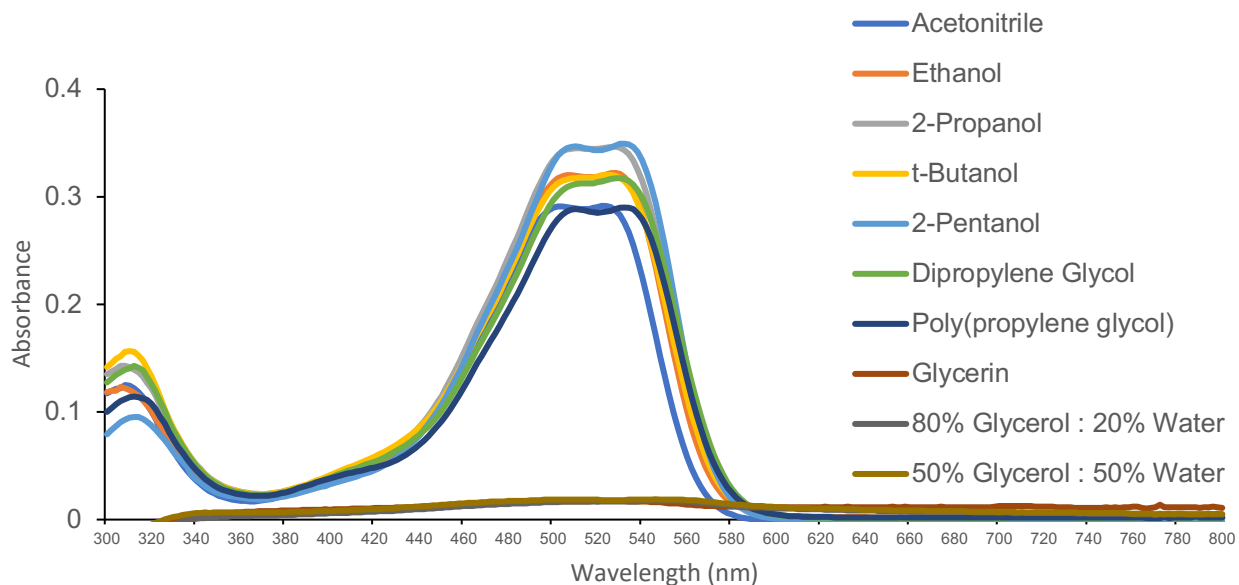
Figure S40: Absorption spectra of a solution of compound 3 in various solvents**Figure S41: Solutions of solutions of compound 3 in various solvents. From left to right: MeCN, IPA, t-BuOH, 2-Pentanol, Polyethylene glycol, Dipropylene glycol, Glycerol, 80% Glycerol-20% H₂O, 50% Glycerol-50% H₂O**

Table S1: Behaviour of azobispyrrole 3 in various media

Medium	Viscosity (cP @ 25 °C)	Dipole Moment (D)	App. Fluor. Intensity	App. Fluor. Color	Observations
Et ₂ O	0.224	1.25	None	-	Fully soluble.
MeCN	0.341	3.44	Moderate	Red	Fine suspension, settles quickly, fluoresces red throughout.
MeOH	0.545	1.6	Weak	Red	Mostly soluble, dark red solution. Over time forms small crystals that fluoresce weakly.
DMSO	1.97	3.9	None	-	Fully soluble, but no apparent fluorescence. Compound crystallizes after some time, leaving solvent colourless.
Diethyl succinate	2.46	2.17	Moderate	Orange	Soluble, but slow to dissolve. Still dissolved after 5 d.
Diethyl adipate	2.78 @ 30 °C	2.4	Moderate	Orange	Soluble, but slow to dissolve. Some crystallization after 5 d.
<i>Tert</i> -BuOH	3.35	1.7	Bright	Red	Forms suspension that settles quickly
Sulfolane	10.1	4.8	Bright	Red	Suspends like in <i>t</i> BuOH yet much more stable; settles only slowly/moderately
Dipropylene glycol	75	1.72	Bright	Orange	Forms excellent stable suspension; only moderate settling after 5 d
PEG-400	101.5	≥3.5	Bright	Orange	Forms excellent stable suspension. Looks macroscopically homogeneous. Only moderate settling after 5 d
Glycerol + EtOH	945 (glycerol)	1.7 (glycerol)	Bright	Red	Forms suspension. Does not interact with glycerol alone (rather, solid floats on it).

Figure S42: Different states of compound 3 under ultraviolet light. Left: solid 3. Suspensions of 3 in A) glycerol-ethanol B) tert-butanol C) dipropylene glycol and D) PEG-400.

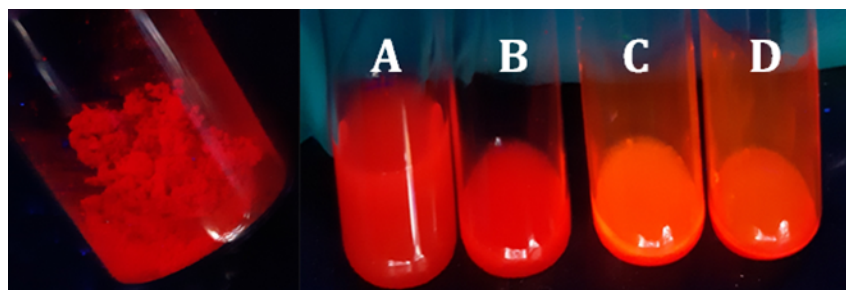


Figure S43: Emission spectra of 3 in PEG at varying concentrations

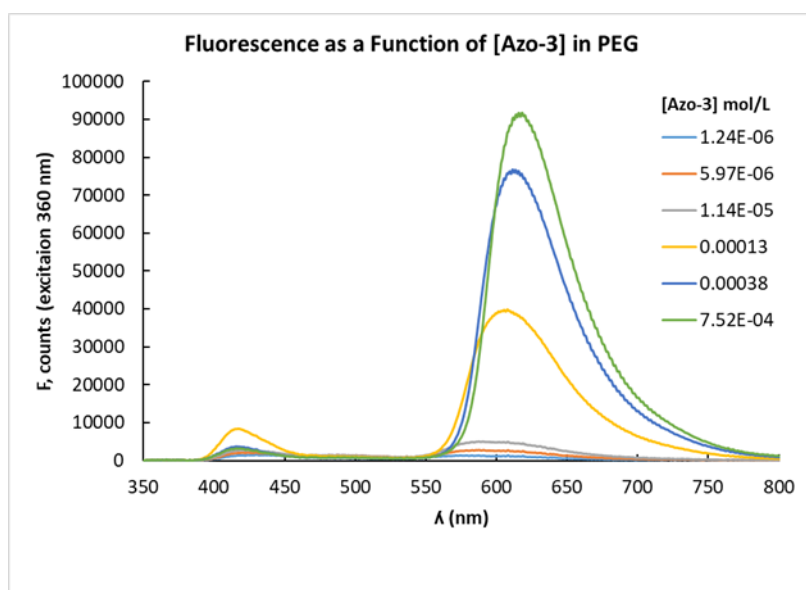


Figure S44: Photograph of visible aggregates formed at 4.0×10^{-4} mol/L **3 in PEG**

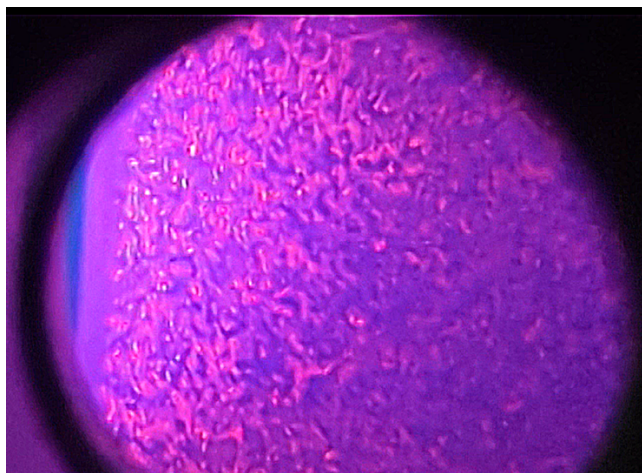


Figure S45: Absorbance spectra for a solution of compound 3 (0.04 mM) in MeOH with increasing amounts of added water

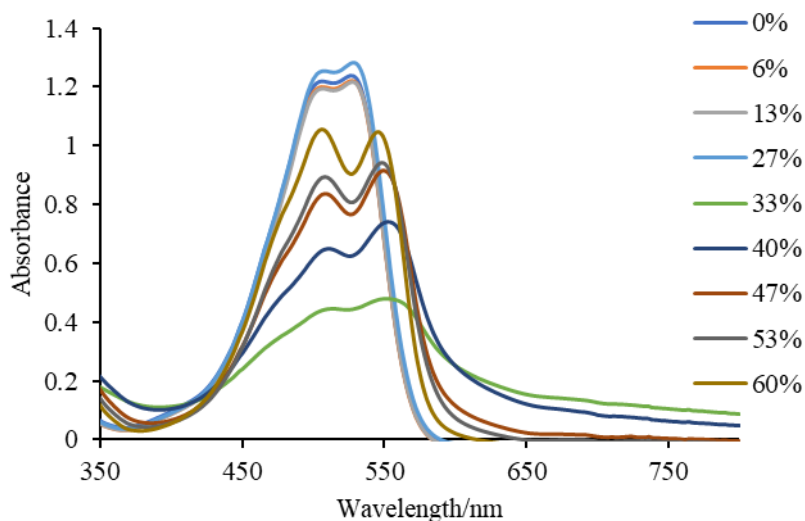


Figure S46: Change in absorbance intensity at 500 nm for a solution of compound 3 (0.04 mM) in MeOH with increasing amounts of added water

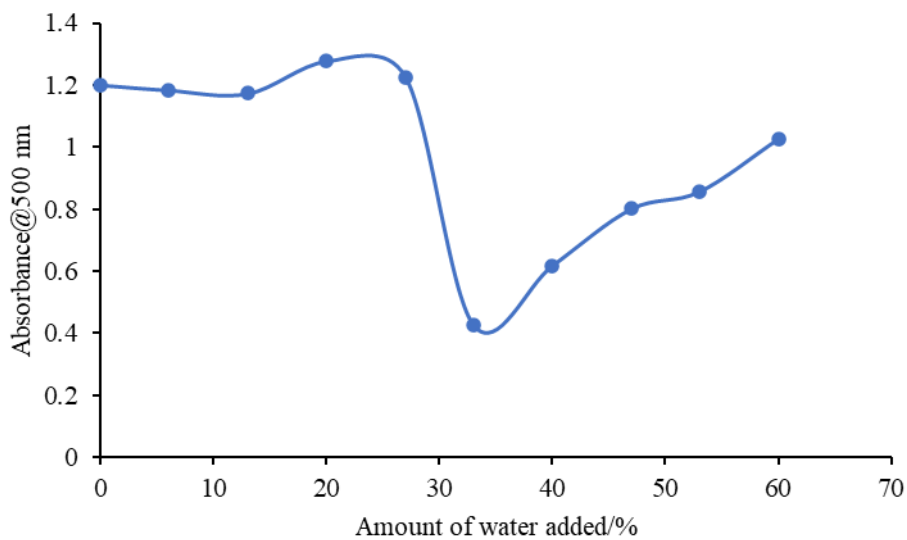


Figure S47: Emission spectra for a solution of compound 3 (0.04 mM) in MeOH with varying amounts of added water (excited at 600 nm)

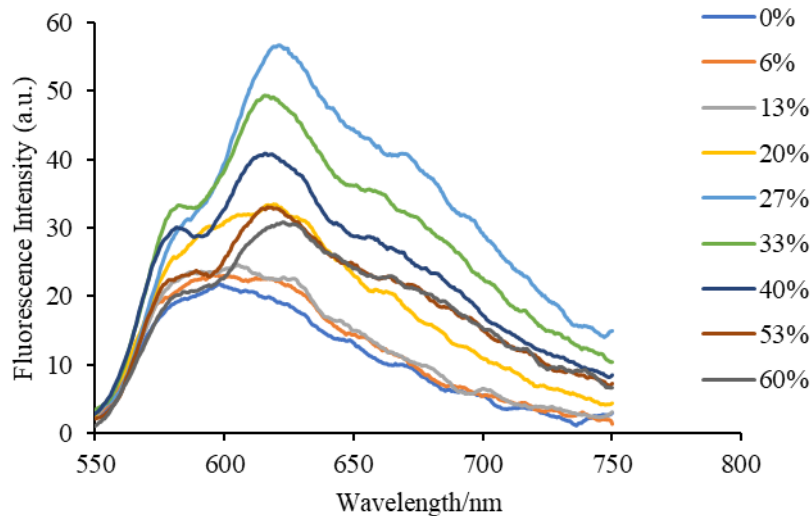


Figure S48: Change in emission intensity at 620 nm (excited at 600 nm) for a solution of compound 3 (0.04 mM) in MeOH with increasing amounts of added water

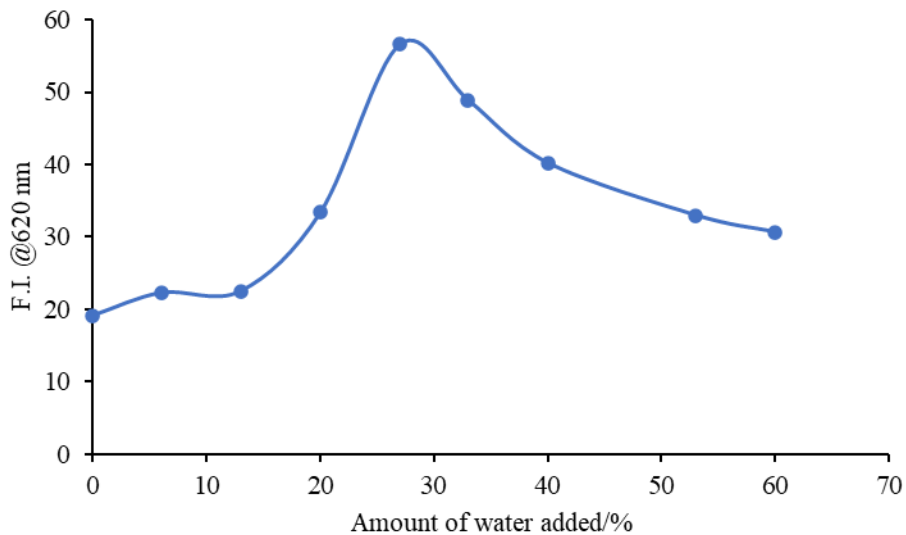
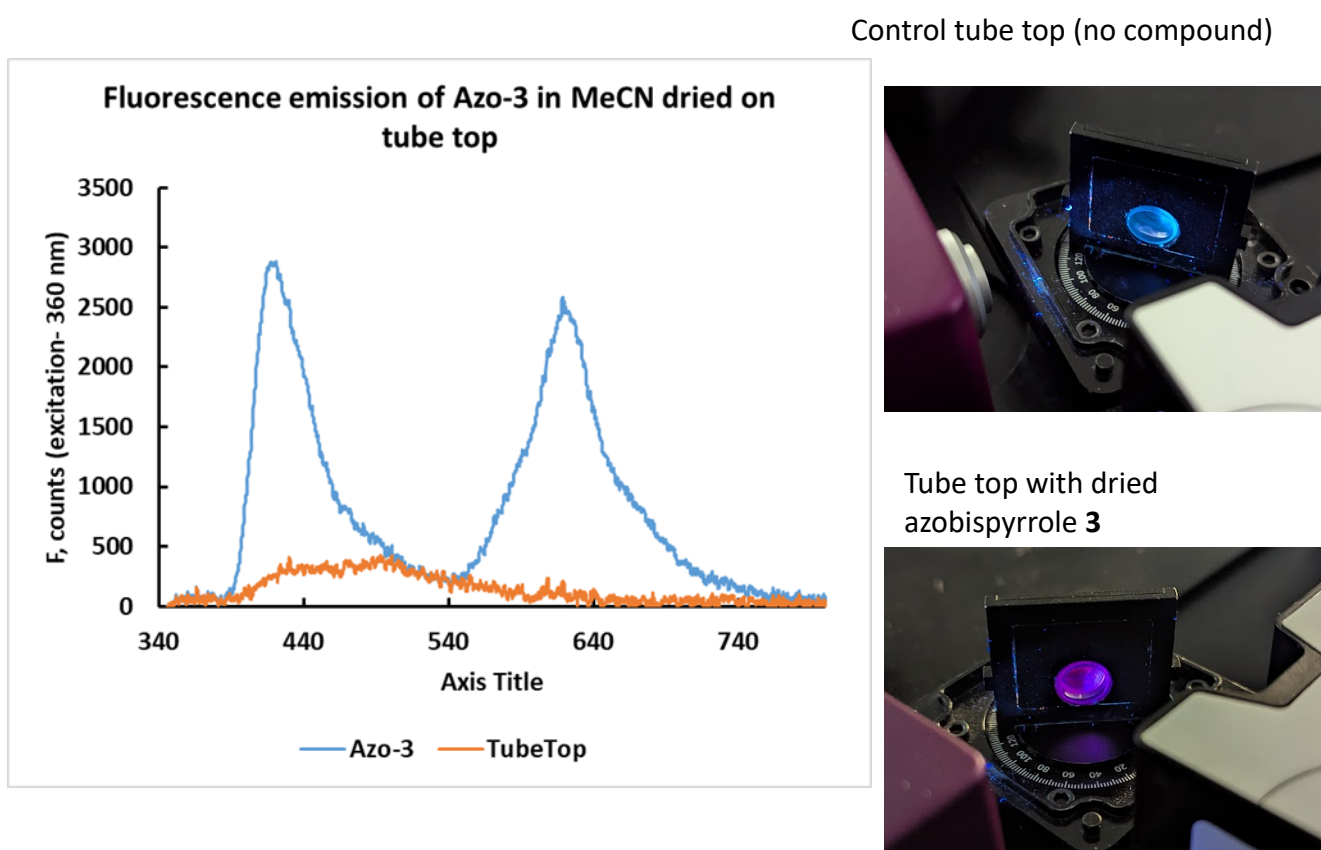


Figure S49: Emission spectra of 3 as solid material dried from solution in MeCN

NMR Spectra

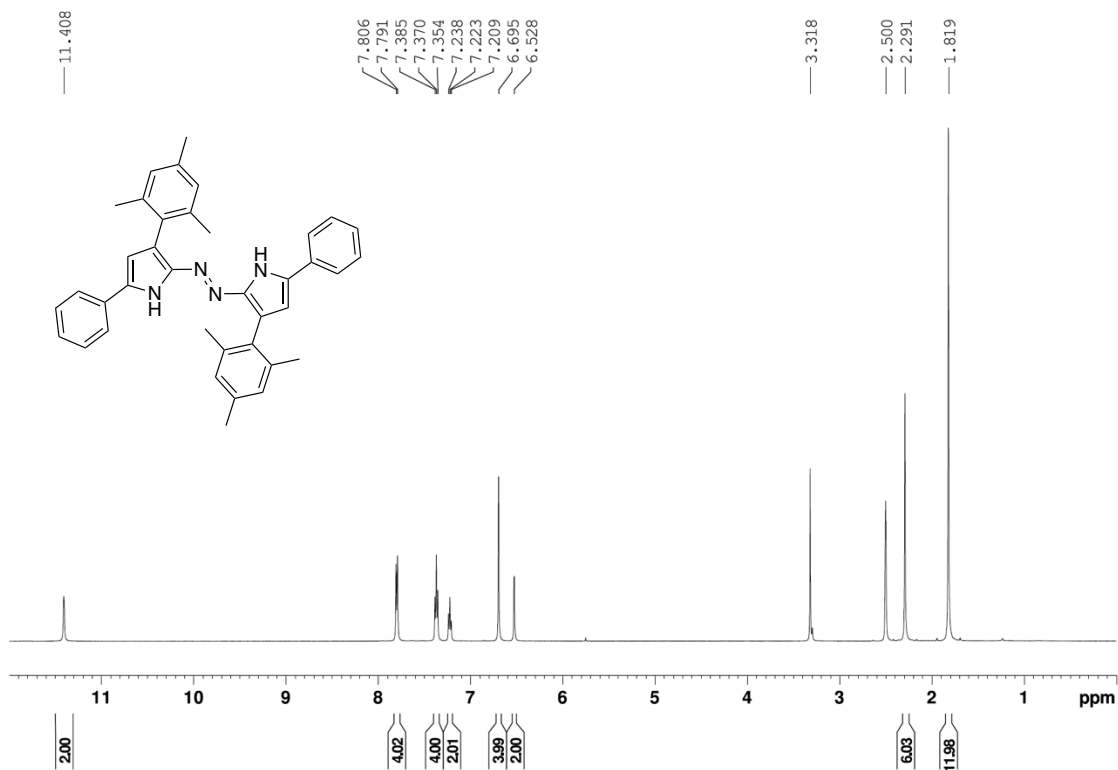
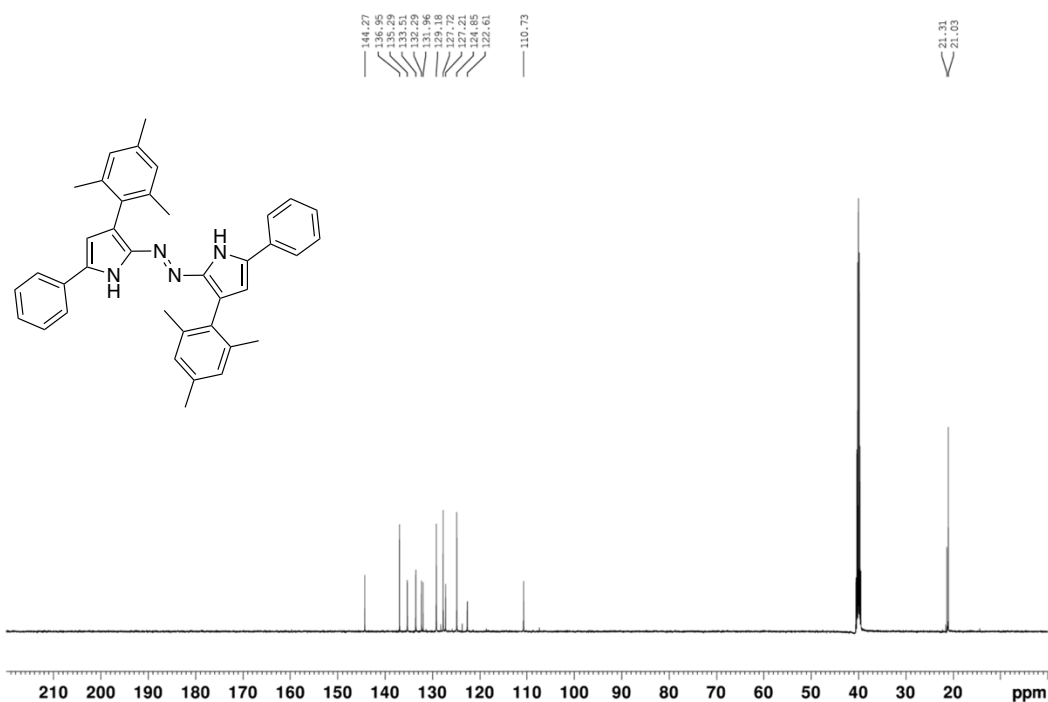
Figure S50: ^1H NMR (500 MHz) spectrum of compound 3 in d_6 -DMSOFigure S51: $^{13}\text{C}\{^1\text{H}\}$ NMR (125 MHz) spectrum of compound 3 in d_6 -DMSO

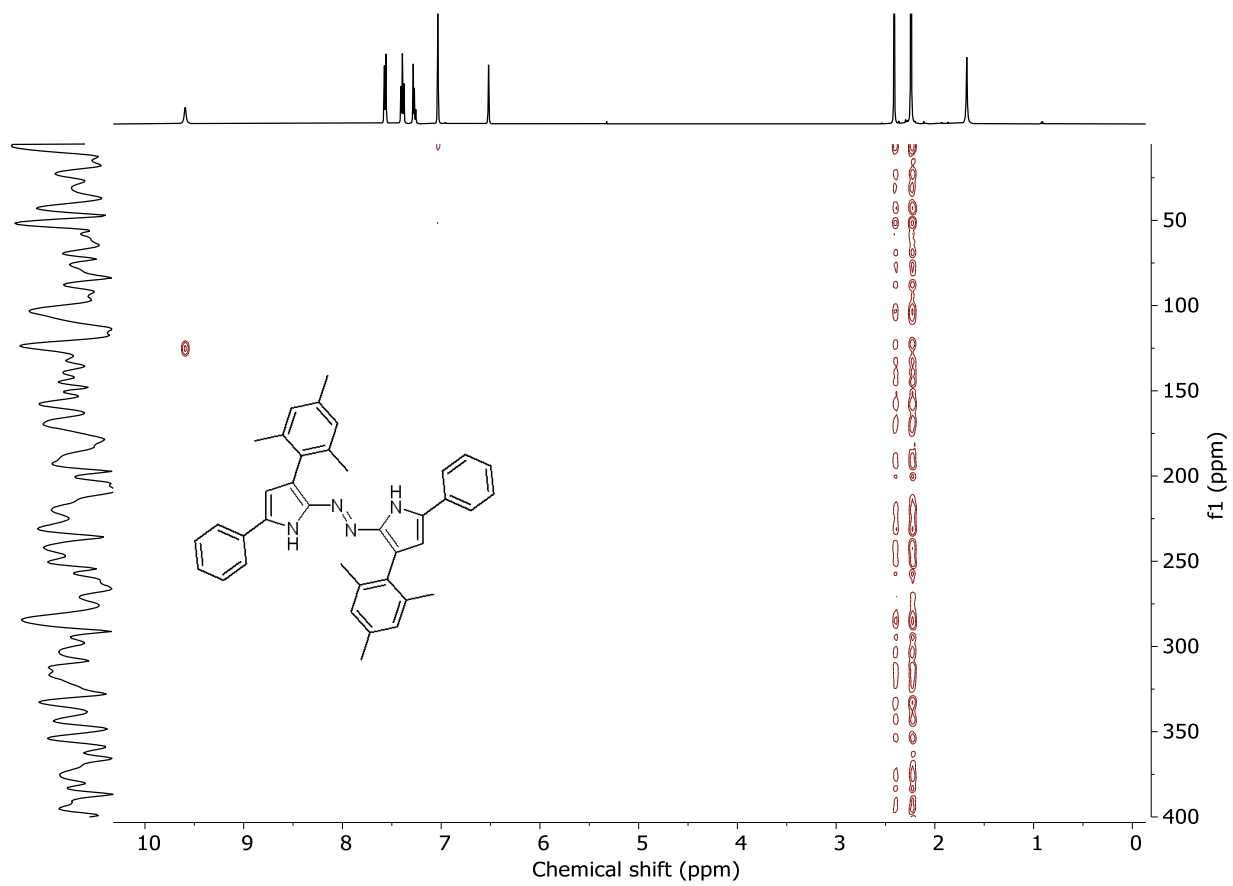
Figure S52: ^1H - ^{15}N HMQC NMR (500 MHz) spectrum of compound 3 in CDCl_3 

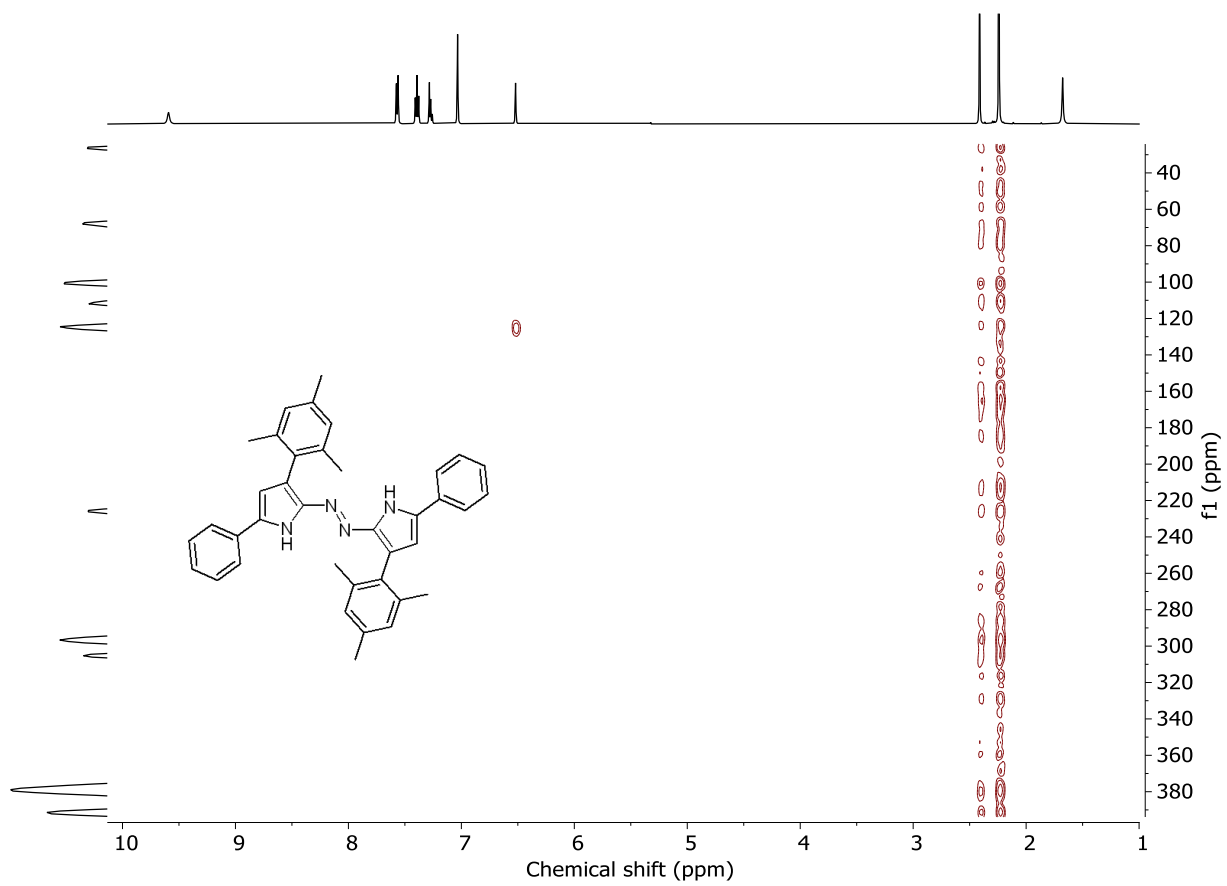
Figure S53: ^1H - ^{15}N HMBC NMR (500 MHz) spectrum of compound 3 in CDCl_3 

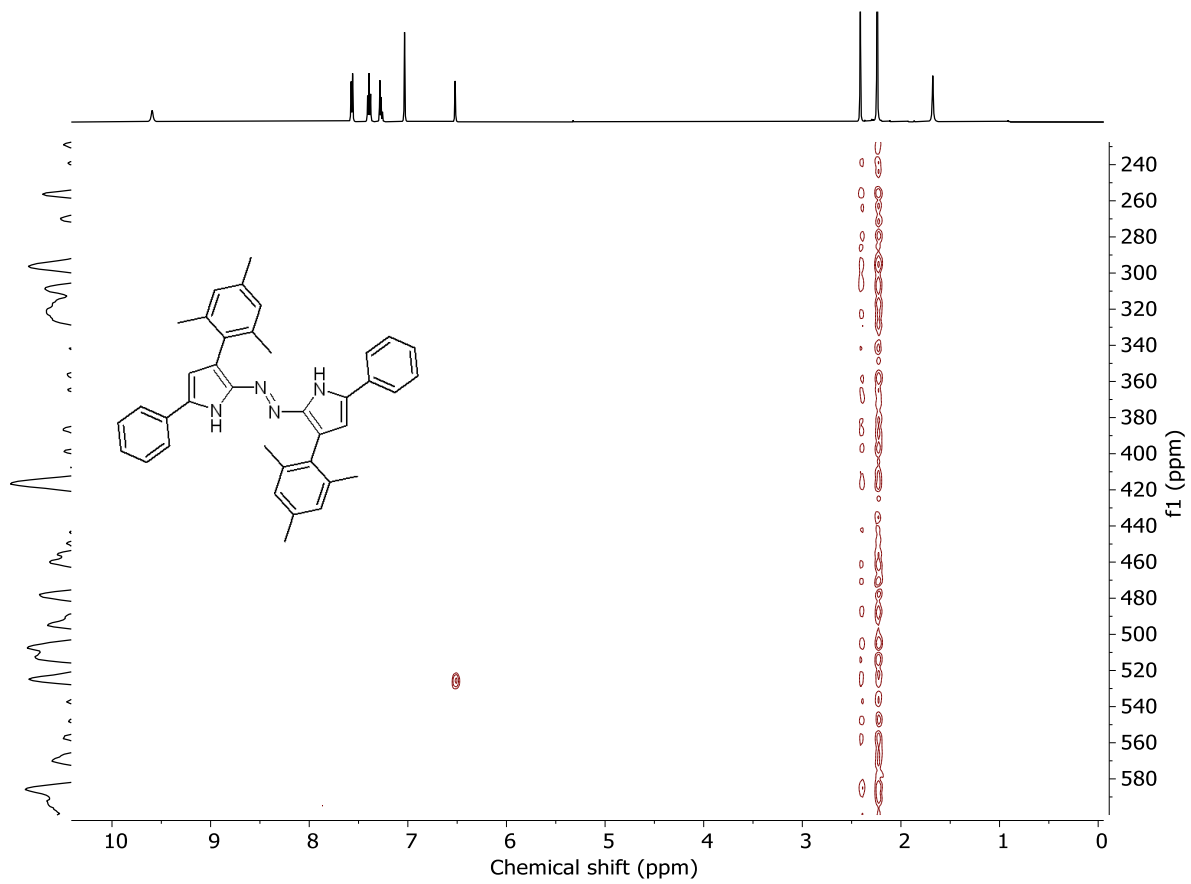
Figure S54: ^1H - ^{15}N HMBC NMR (500 MHz) spectrum of compound 3 in CDCl_3 

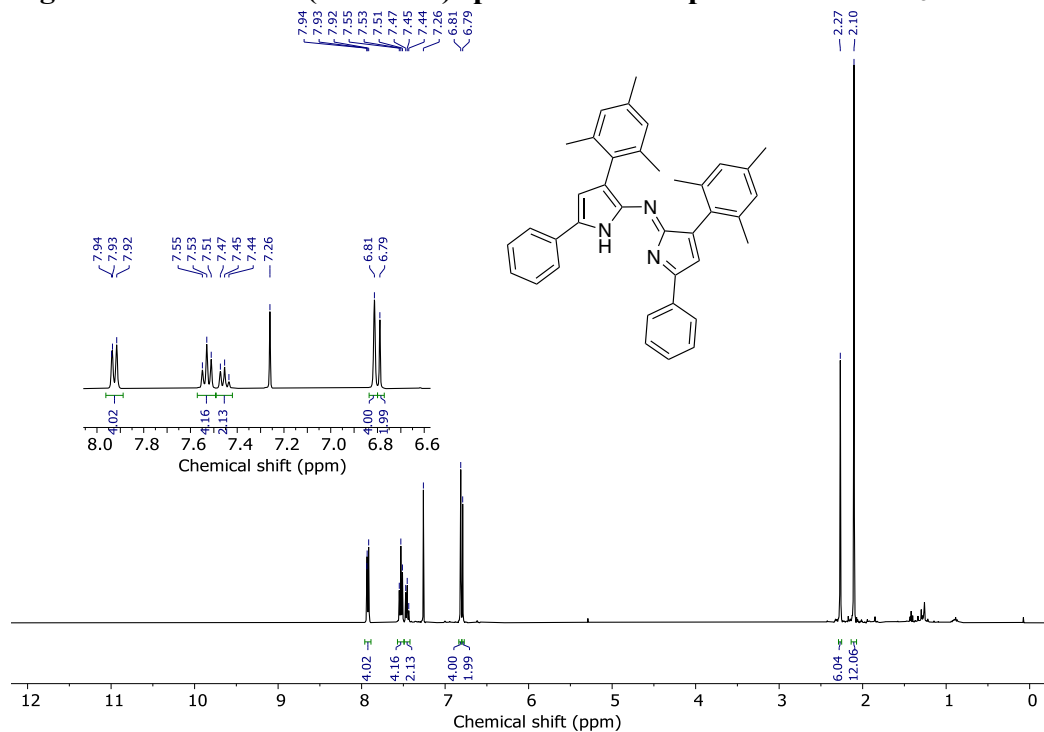
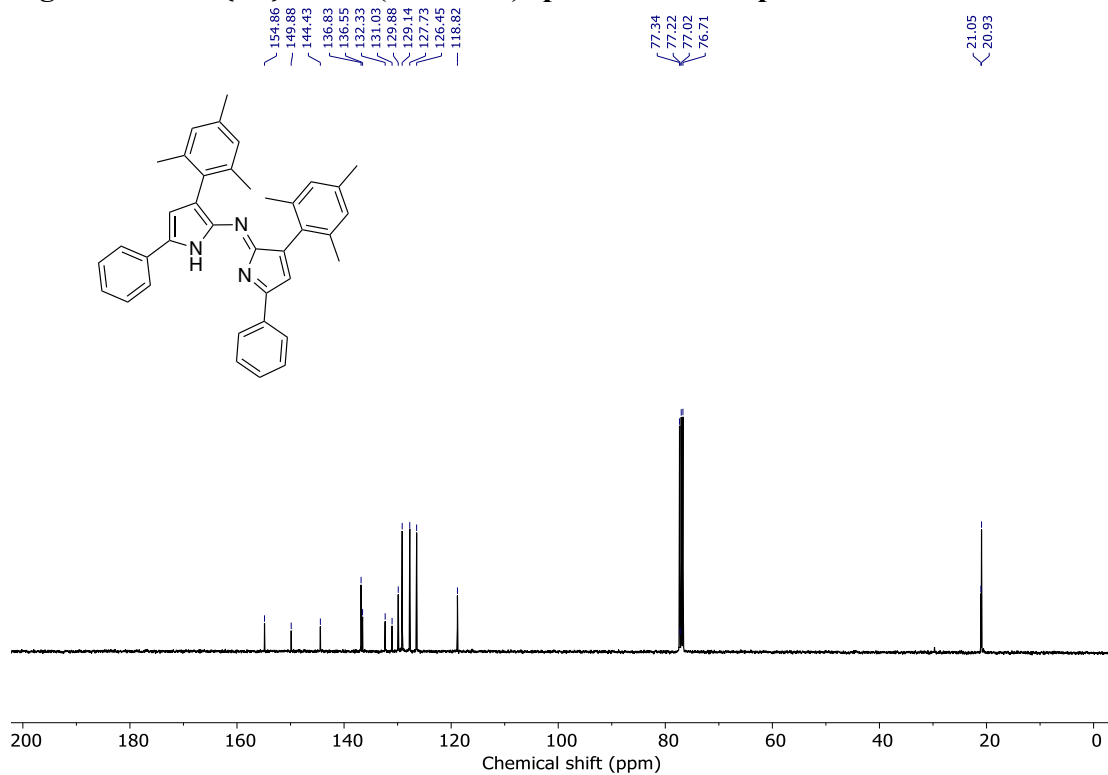
Figure S55: ^1H NMR (500 MHz) spectrum of compound 4 in CDCl_3 Figure S56: $^{13}\text{C}\{^1\text{H}\}$ NMR (100 MHz) spectrum of compound 4 in CDCl_3 

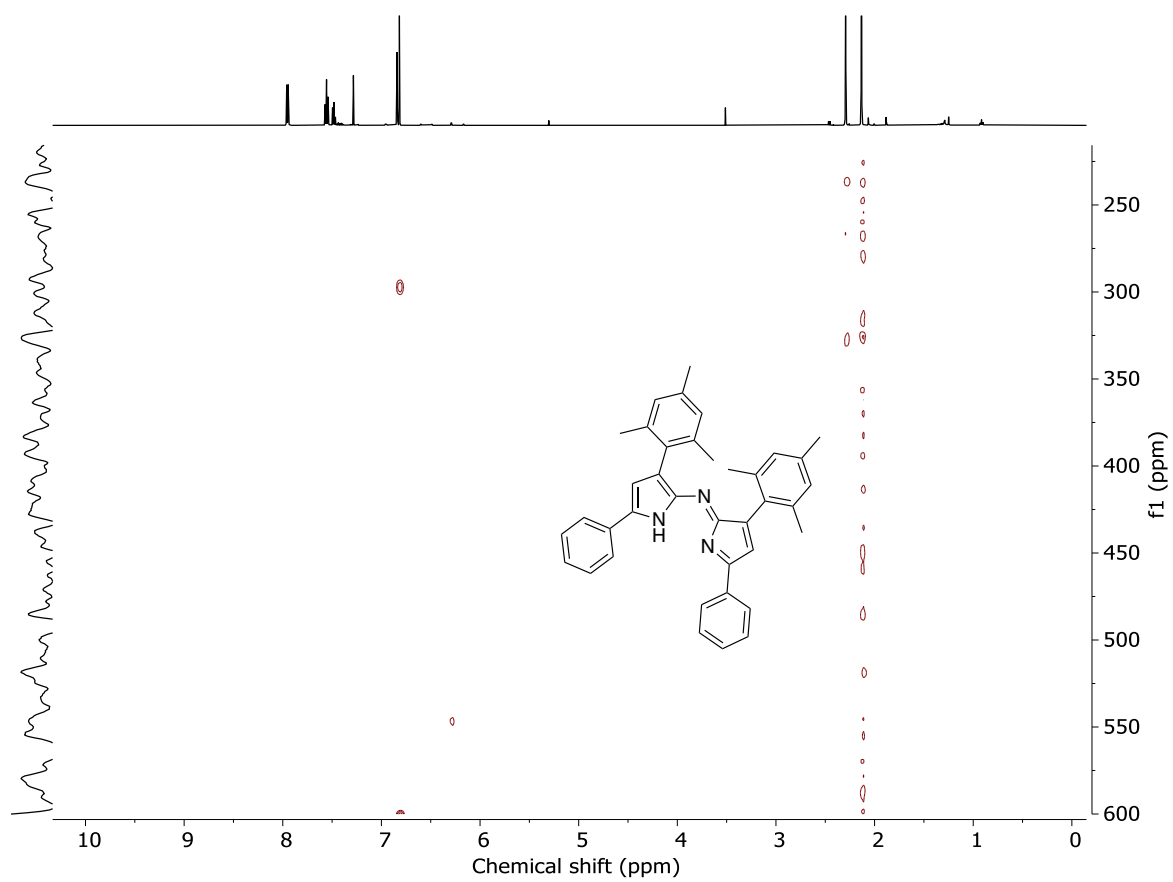
Figure S57: ^1H - ^{15}N HMBC NMR (500 MHz) spectrum of compound 4 in CDCl_3 

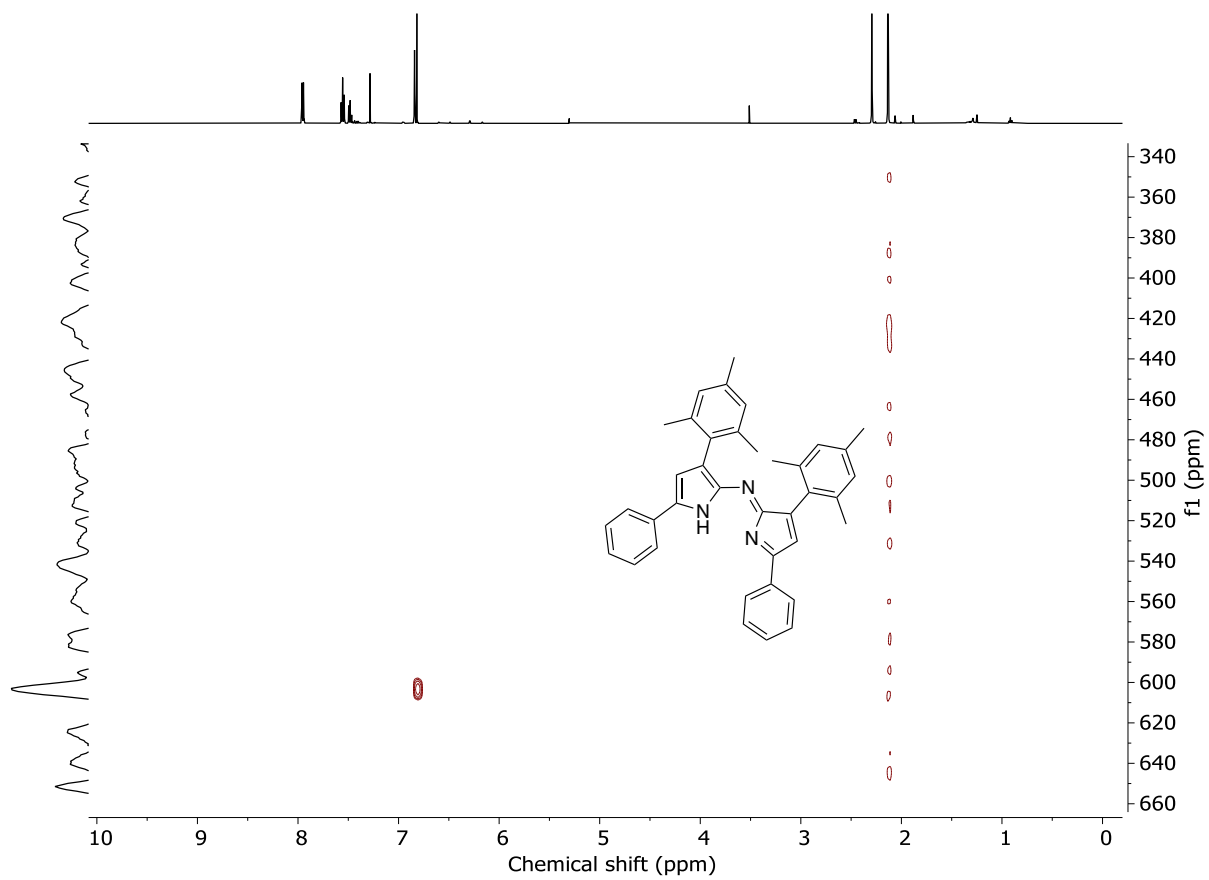
Figure S58: ^1H - ^{15}N HMBC NMR (500 MHz) spectrum of compound 4 in CDCl_3 

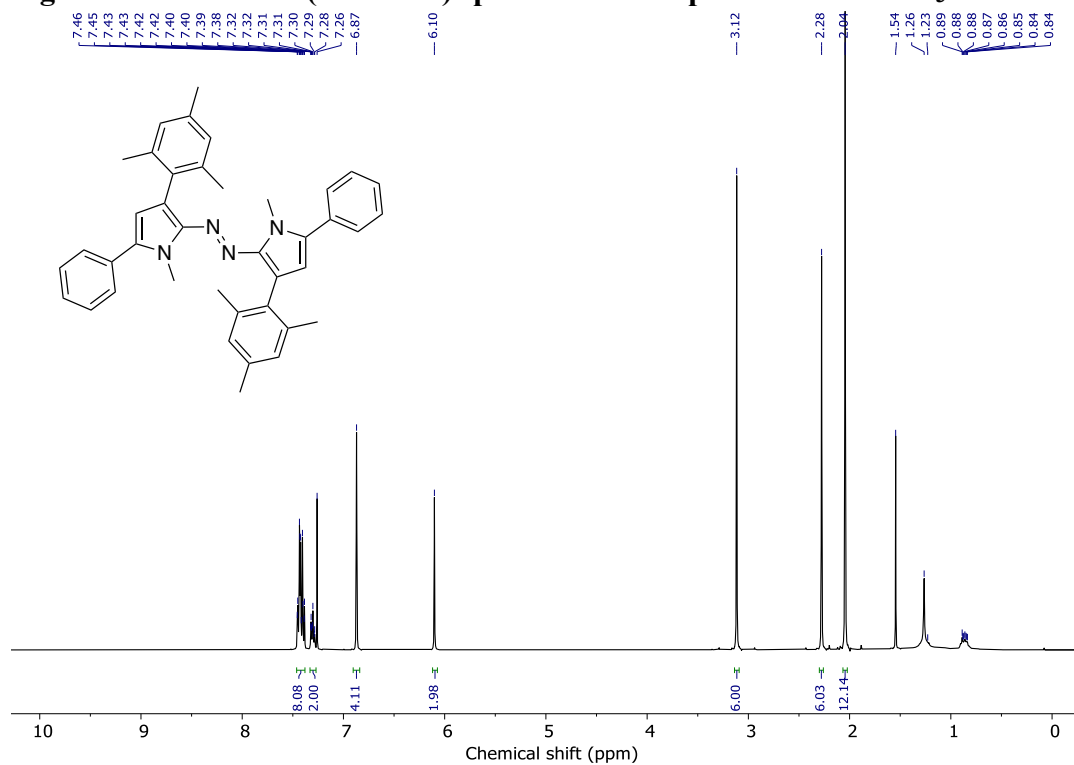
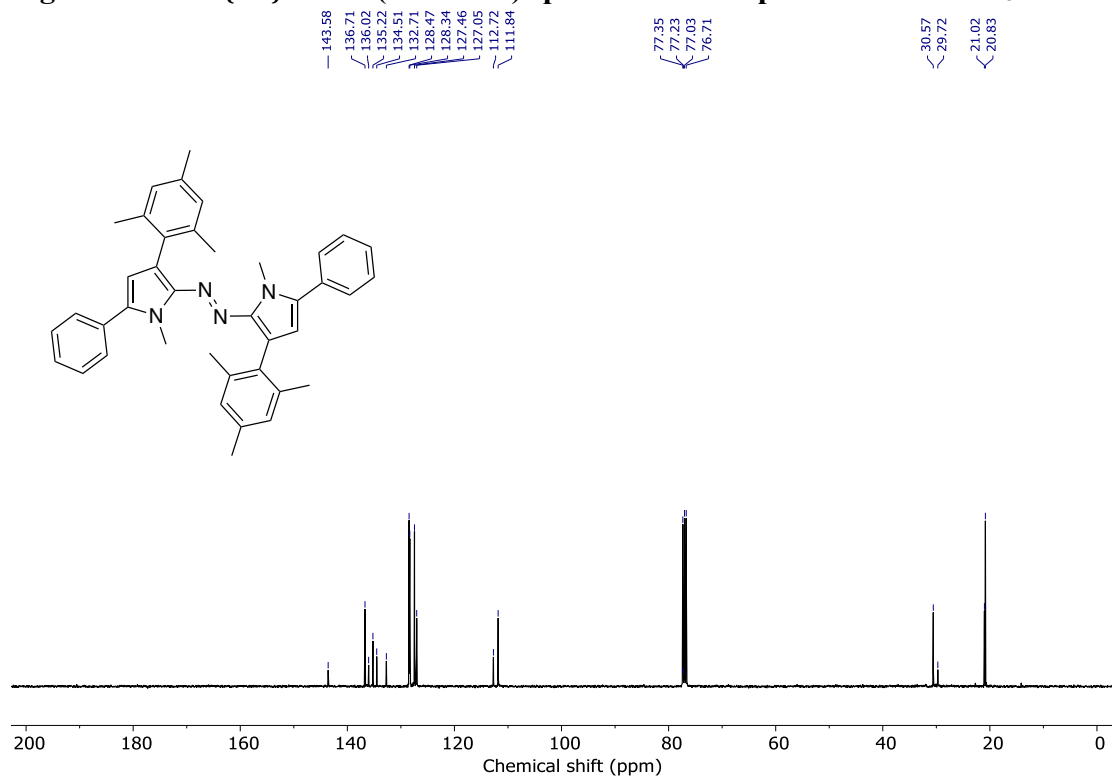
Figure S59: ^1H NMR (500 MHz) spectrum of compound 5a in CDCl_3 Figure S60: $^{13}\text{C}\{^1\text{H}\}$ NMR (100 MHz) spectrum of compound 5a in CDCl_3 

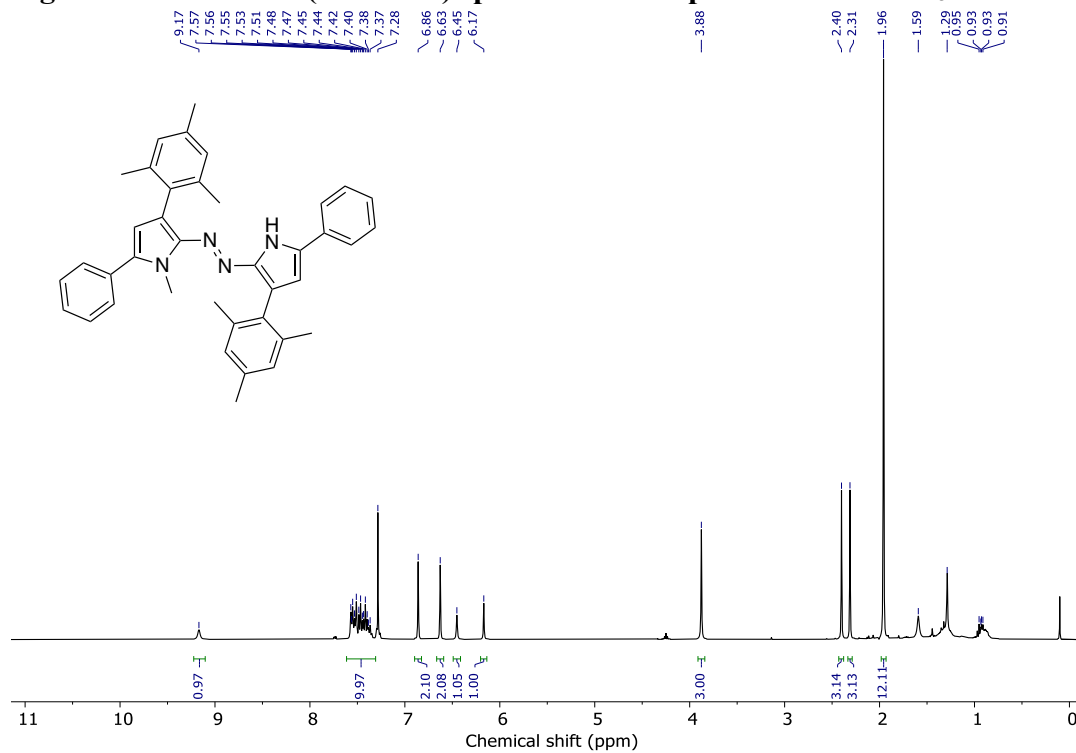
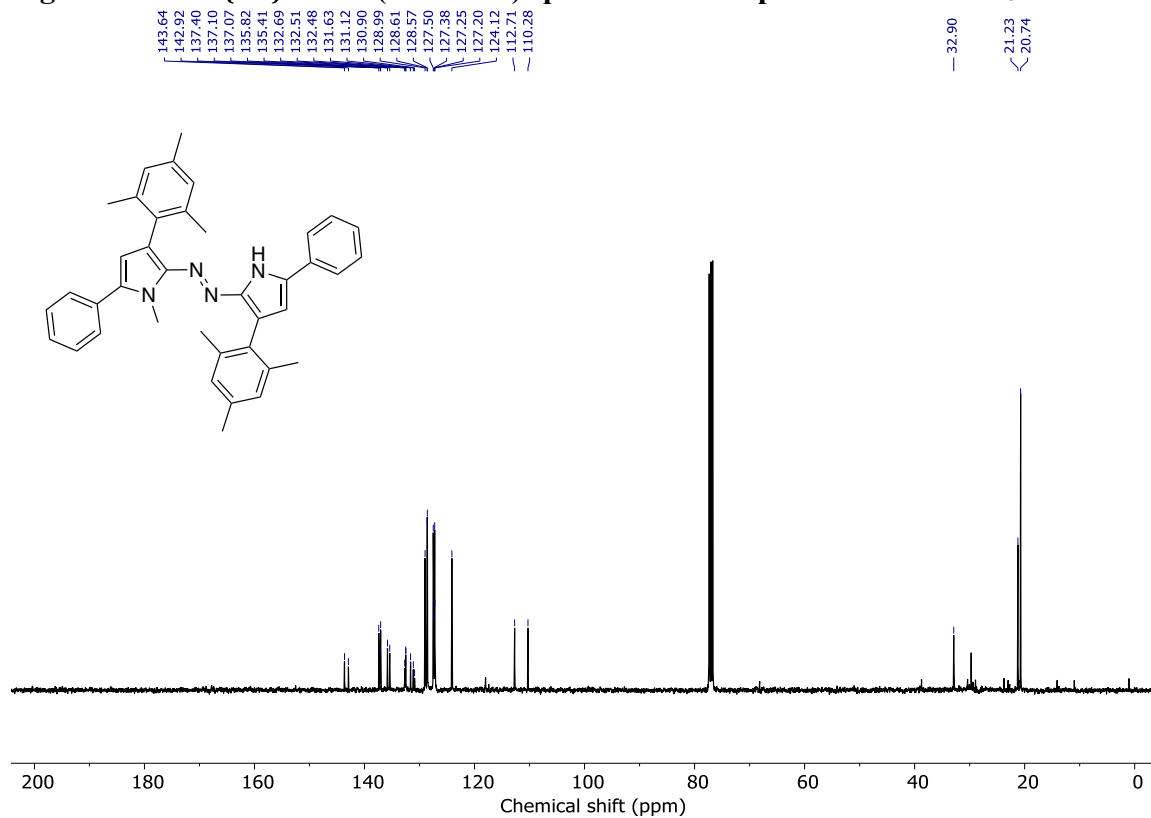
Figure S61: ^1H NMR (500 MHz) spectrum of compound 5b in CDCl_3 Figure S62: $^{13}\text{C}\{^1\text{H}\}$ NMR (100 MHz) spectrum of compound 5b in CDCl_3 

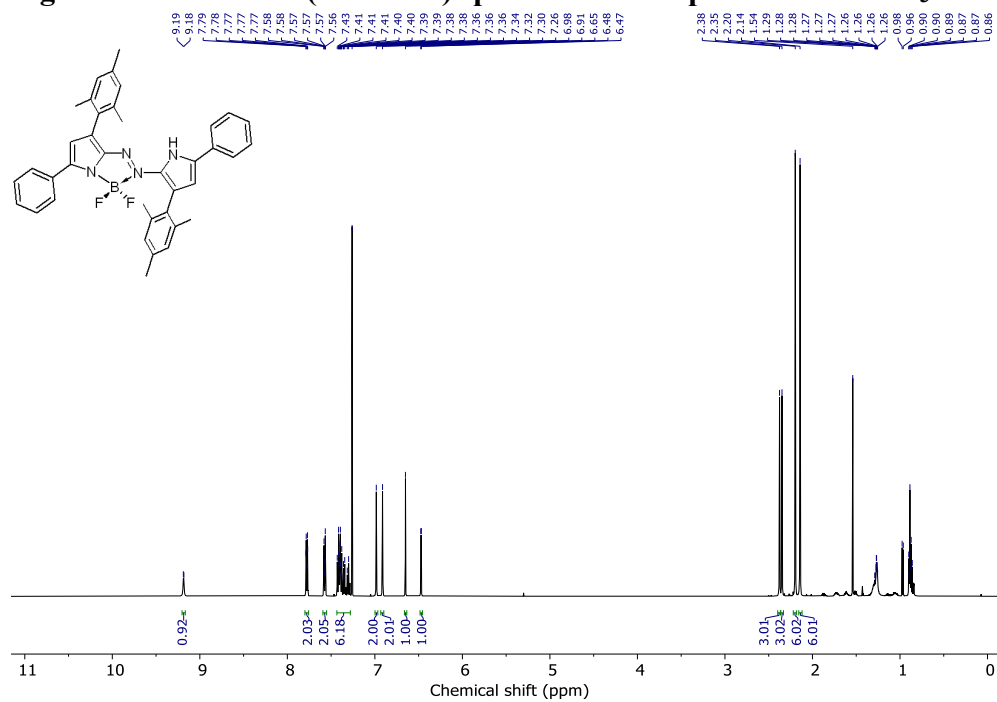
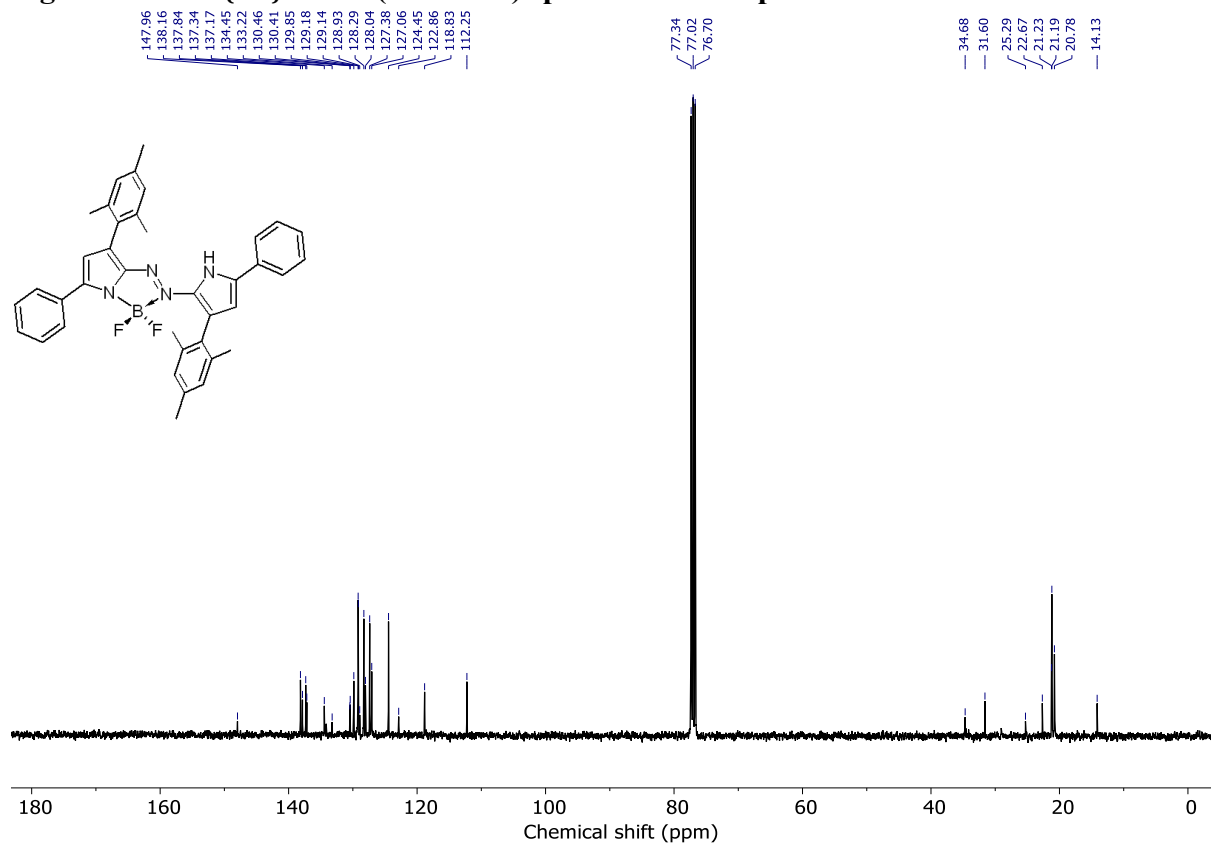
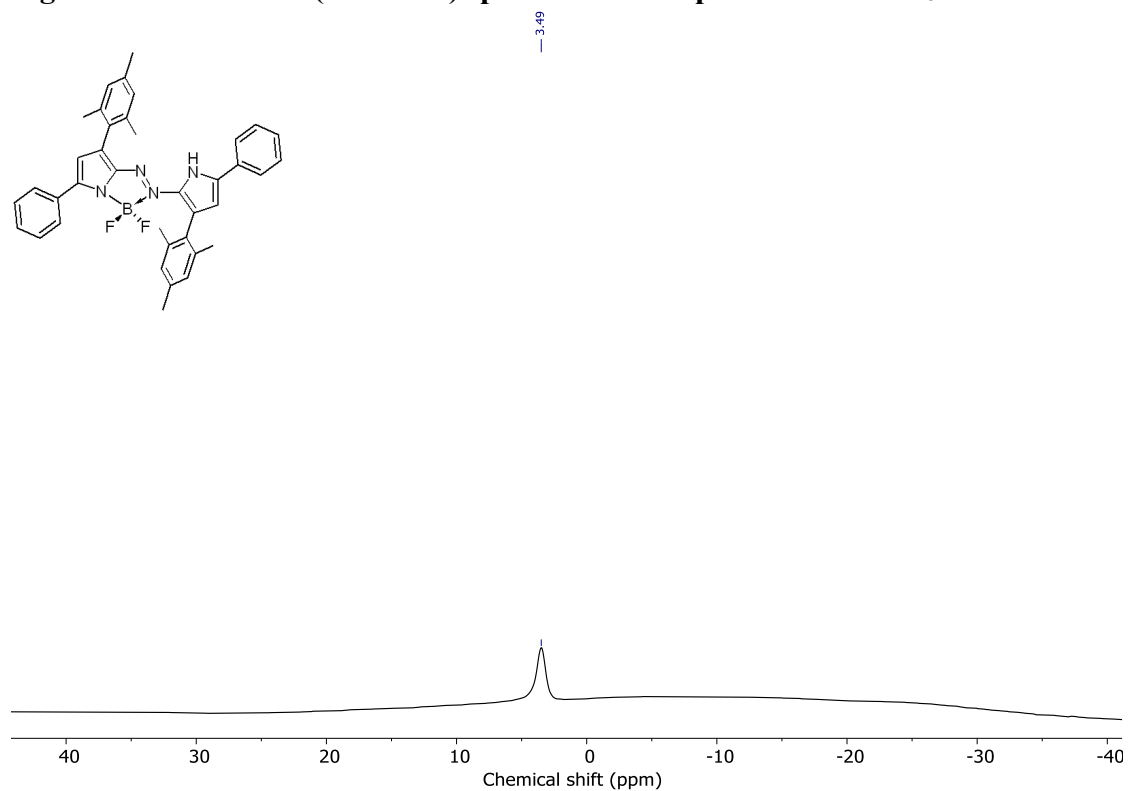
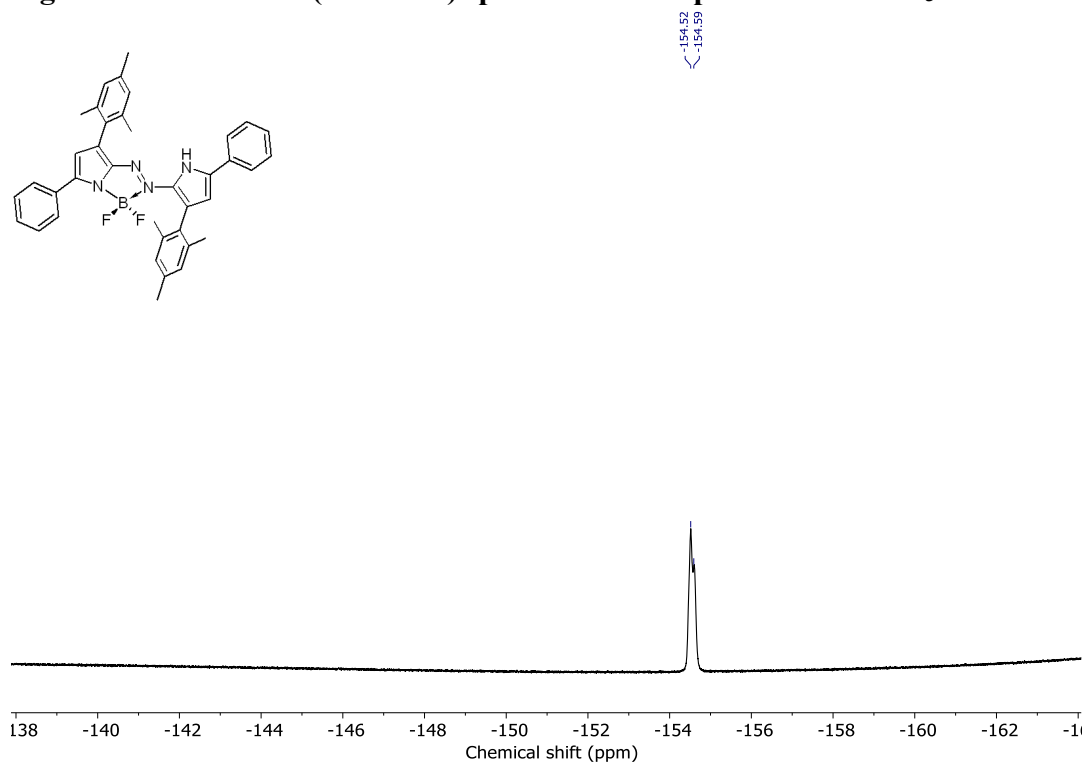
Figure S63: ^1H NMR (500 MHz) spectrum of compound 6 in CDCl_3 Figure S64: $^{13}\text{C}\{^1\text{H}\}$ NMR (100 MHz) spectrum of compound 6 in CDCl_3 

Figure S65: ^{11}B NMR (160 MHz) spectrum of compound 6 in CDCl_3 Figure S66: ^{19}F NMR (470 MHz) spectrum of compound 6 in CDCl_3 

X-ray Crystallography

The crystal chosen was attached to the tip of a MicroLoop with paratone-N oil. Measurements were made on a Bruker D8 VENTURE diffractometer equipped with a PHOTON III CMOS detector using monochromated Mo K α radiation ($\lambda = 0.71073 \text{ \AA}$) from an Incoatec microfocus sealed tube at 150 K.⁴ The initial orientation and unit cell were indexed using a least-squares analysis of the reflections collected from a complete 180° phi-scan, 5 seconds per frame and 1° per frame. For data collection, a strategy was calculated to maximize data completeness and multiplicity, in a reasonable amount of time, and then implemented using the Bruker Apex 4 software suite.⁴ The data were collected with 30 sec frame times for **3**, 20 sec for **5a** and 60 sec for **6** (0.5° per frame in all cases) and the crystal to detector distance was set to 4 cm. Cell refinement and data reduction were performed with the Bruker SAINT⁵ software, which corrects for beam inhomogeneity, possible crystal decay, and Lorentz and polarisation effects. A multi-scan absorption correction was applied (SADABS⁶). The structures were solved using SHELXT-2014^{7,8} and were refined using a full-matrix least-squares method on F^2 with SHELXL-2019.^{7,8} The refinements were unremarkable. The non-hydrogen atoms were refined anisotropically. The hydrogen atoms bonded to carbon were included at geometrically idealized positions and were allowed to ride on the heavy atoms to which they were bonded. The isotropic thermal parameters of these hydrogen atoms were fixed at $1.2U_{eq}$ of the parent carbon atom or $1.5U_{eq}$ for methyl hydrogens. The positions of the hydrogen atoms bonded to nitrogen and oxygen were located in near final Fourier difference maps. They were included in the refinement with the H(N) atoms refined isotropically and the H(O) atoms having U_{isoH} equal to $1.5U_{eq}$ of the parent oxygen atom. Where necessary geometric restraints were placed on the N-H bond lengths to keep them reasonable.

Azobispyrrole **3**

Data was collected and integrated to a maximum resolution of 0.80 \AA ($\theta_{max} = 26.40^\circ$). Two reflections (0 -2 2 and -2 -2 2) were removed from the final refinement because of poor agreement between F_{obs}^2 and F_{calc}^2 .

The compound crystallized in the centrosymmetric Triclinic space group $\overline{P1}$ with one half of each of two unique molecules in the asymmetric unit. There was also one molecule of water found in the asymmetric unit.

In the final checkcif file there were two unexpected level B alerts. Both of these were “D-H Bond Without Acceptor” alerts involving the O-H groups of the water molecule. This is not true. Each of the OH groups participates in an intermolecular hydrogen bond with the acceptor being electron density in one of the mesityl rings in the structure. The result is that the two complete molecules wrap around the central water molecule, with the OH groups hydrogen bonded to mesityl rings in each of them. The data for these interactions are given in the table of hydrogen bonds (Table S2) and they are shown in the hydrogen bonding diagram included for this structure. This type of hydrogen bonding is not recognized in the routines Platon uses to run the checkcif program.

***N,N*-Dimethylated azo-bispyrrole 5a**

Data was collected and integrated to a maximum resolution of 0.75 Å ($\theta_{\max} = 28.28^\circ$). One reflection (1 2 0), which was partially obscured by the beam stop, was removed from the final refinement because of poor agreement between F_{obs}^2 and F_{calc}^2 .

The unit cell found during data processing was *C*-centered monoclinic. However, no reasonable space group could be determined from the systematic absences and no reasonable solution could be found for the structure in any monoclinic space group. Processing the data using a smaller triclinic cell gave good statistics and an immediate solution was found in space group $\overline{P1}$. Twin Rot Mat from the program Platon⁹ showed that the crystal was a pseudo-merohedral twin, with the triclinic cell resembling a *C*-centered monoclinic cell. Addition of the twin law: -1 0 0 0 -1 0 -1 0 and refinement of BASF (0.4851(7)) gave excellent results. In the centrosymmetric triclinic space group *P*-1 there are four unique molecules in the asymmetric unit. There was no solvent found in the lattice and no disorder in any of the four molecules.

Once the triclinic refinement was complete, attempts were made to search for higher metric symmetry. The positions of the molecules in the triclinic cell were checked to make sure that no two were related by translations of one half along any axis. The triclinic cell and its contents were transformed to the higher symmetry *C*-centered cell. Attempted refinements were unsuccessful. Overlays of the possible combinations of all four molecules were made and none were identical. All of this suggests that the choice of refining this structure as a pseudo-merohedral twin in the triclinic space group $\overline{P1}$ is the correct one. Still there is a chance that the correct monoclinic solution for this structure has just not been located.

Because of the large number of atoms in the asymmetric unit, conventional consecutive numbering through all four molecules was not possible (for the methyl hydrogen atoms in particular). Instead, each molecule was placed in a separate residue (RESI1 to RESI4) and the atoms numbered consecutively (N1-N4 and C1-C40) using the same order and labels in all four residues.

BF₂ complex 6

Data was collected and integrated to a resolution of 0.75 Å ($\theta_{\max} = 28.28^\circ$) to give a full set of data of reasonable completeness and intensity. One reflection (3 3 0) was removed from the final refinement because of poor agreement between F_{obs}^2 and F_{calc}^2 .

The compound was found to crystallize in the non-centrosymmetric orthorhombic space group *Pna*2₁, with one molecule of product and one molecule of acetonitrile solvate comprising the asymmetric unit. There was no disorder observed in the structure. There are no chiral centers in the molecule so the non-centrosymmetric space group must occur for other reasons.

During the course of the refinement, the occupancies of all of the heavy atoms were checked by refining their values. Most of the atomic occupancies refined to one as expected, however, the final occupancies of the atoms in the BF₂ group refined to slightly lower values. The average occupancy of these three atoms refined to 94 % and the statistics of the refinement improved slightly when these lower occupancies were included. Since this compound was found to be moisture sensitive, both in solution and in the solid state, it is likely that a small amount of decomposition of the

crystals occurred before the data collection was begun. No attempt was made to model the disorder, and the results with all atoms having full occupancies have been reported here.

The absolute structure of the crystal was not well determined. The value of the absolute structure parameter from the Shelxl refinement is 0.23(17). If the structure is treated as an inversion twin and the BASF parameter refined, the result is 0.1(7), while if it is inverted and refined BASF becomes 0.9(7). The program Platon⁹ was used to calculate the Hooft parameter ($y = 0.25(16)$) which is in good agreement with the absolute value determined using Shelxl. All of these results suggest that the correct absolute configuration has been assigned to the structure, even if the values themselves are not well determined.

All diagrams were prepared using the program Mercury CSD 2021.1.0.¹⁰ The crystallographic data has been deposited with the Cambridge Crystallographic Data Centre. CCDC 2410353-2410355 contain the supplementary crystallographic data for this paper. The individual number for each structure is given in Table S1. These data can be obtained, free of charge, via <https://www.ccdc.cam.ac.uk/structures> or from the Cambridge Crystallographic Data Centre, 12 Union Road, Cambridge CB2 1EZ, UK (Fax: 44-1223-336033 or e-mail: deposit@ccdc.cam.ac.uk).

Table S2: Crystal data and structure refinement details.

	3	5a	6
Identification code	3	5a	6
CCDC deposit number	2410353	2410354	2410355
Empirical formula	C ₃₈ H ₃₈ N ₄ O	C ₁₆₀ H ₁₆₀ N ₁₆	C ₄₀ H ₃₈ BF ₂ N ₅
Formula weight	566.72	2307.03	637.56
Crystal system	Triclinic	Triclinic	Orthorhombic
Space group	<i>P</i> -1	<i>P</i> -1	<i>Pna</i> 2 ₁
Unit cell dimensions (Å and °)	<i>a</i> = 10.6572(4) <i>b</i> = 12.3917(5) <i>c</i> = 12.8250(5) α = 105.7410(14) β = 95.3783(14) γ = 104.4287(14)	<i>a</i> = 19.2320(8) <i>b</i> = 19.9165(7) <i>c</i> = 19.9108(8) α = 68.1270(14) β = 74.0072(15) γ = 73.9936(14)	<i>a</i> = 22.8308(5) <i>b</i> = 19.6331(5) <i>b</i> = 19.6331(5) α = 90 β = 90 γ = 90
Volume (Å ³)	1554.92(11)	6674.3(5)	3459.06(15)
<i>Z</i>	2	2	4
Density (calculated, Mg/m ³)	1.210	1.148	1.224
Absorption coefficient (mm ⁻¹)	0.074	0.068	0.080
F(000)	604	2464	1344
Crystal size (mm ³)	0.153x0.039x0.024	0.135x0.118x0.063	0.350x0.080x0.042
Theta range of data (°)	2.003 to 26.396	1.826 to 28.278	2.064 to 28.283
Index ranges (<i>h</i> , <i>k</i> , <i>l</i>)	-13/13, -15/15, -16/16	-25/25, -26/26, -26/26	-30/30, -26/26, -10/10
Reflections collected	66976	415165	54194
Independent reflections	6366	33105	8321
R(int)	0.0759	0.0624	0.0364
Completeness to 25.242° (%)	99.9	100.0	99.9
Max. and min. transmission	0.7454 and 0.6991	0.7457 and 0.7059	0.7468 and 0.6798
Data / restraints / parameters	6366 / 0 / 408	33105 / 0 / 1586	8321 / 2 / 444
Goodness-of-fit on F ²	1.085	1.159	1.066
Final R indices [<i>I</i> > 2σ(<i>I</i>)]	R1 = 0.0513 wR2 = 0.1209	R1 = 0.0495 wR2 = 0.1199	R1 = 0.0374 wR2 = 0.0991
R indices (all data)	R1 = 0.0848 wR2 = 0.1477	R1 = 0.0781 wR2 = 0.1519	R1 = 0.0403 wR2 = 0.1016
Absolute structure parameter	n.a.	n.a.	0.23(17)
Largest diff. peak and hole (e.Å ⁻³)	0.262 and -0.267	0.252 and -0.284	0.180 and -0.162

Table S3: Hydrogen bonds [\AA and $^\circ$].

D-H...A	d(D-H)	d(H...A)	d(D...A)	\angle (DHA)
3				
O(1)-H(1O)...Cg1#1	0.86(3)	2.47(3)	3.252(2)	151(2)
O(1)-H(2O)...Cg2#2	0.90(3)	2.49(3)	3.297(2)	151(2)
N(1)-H(1N)...O(1)	0.89(3)	2.11(3)	3.000(2)	176(3)
N(1)-H(1N)...N(2)#1	0.89(3)	2.58(3)	2.733(2)	90.1(18)
N(3)-H(3N)...O(1)	0.91(3)	2.12(3)	3.019(2)	172(2)
N(3)-H(3N)...N(4)#2	0.91(3)	2.53(3)	2.719(2)	92.3(19)
5a				
N(1)-H(1N)...N(5)	0.83(2)	2.30(2)	3.027(3)	146(3)
N(1)-H(1N)...N(3)	0.83(2)	2.42(3)	2.658(2)	97.7(19)

Symmetry transformations used to generate equivalent atoms:

#1 $-x, -y, -z$ #2 $-x, -y+1, -z+1$

Cg1	ring centroid	C5 to C10	position	0.19863(8)	-0.04274(7)	-0.30925(7)
Cg2	ring centroid	C24 to C29		0.19202(8)	0.62968(7)	0.87156(7)

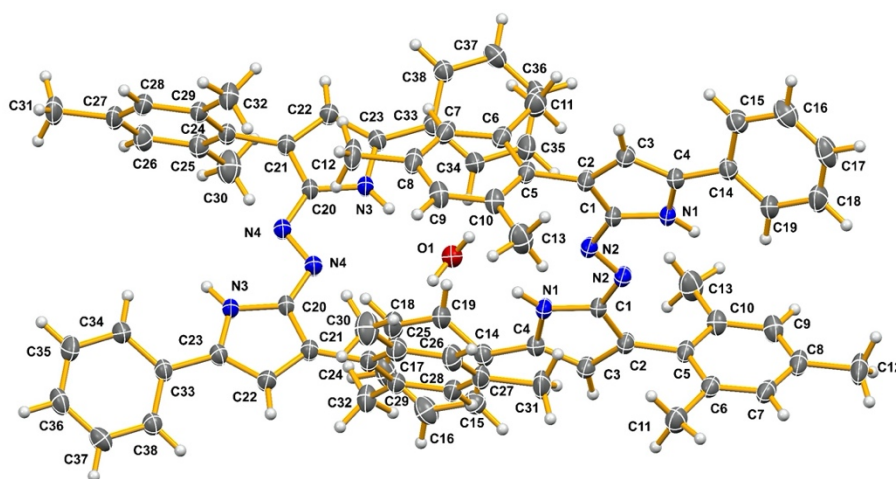


Figure S67: Structure of compound **3** with full labelling, including one molecule of hydration. Thermal ellipsoids have been drawn at the 50% probability level. Hydrogen atoms are included but have not been labelled.

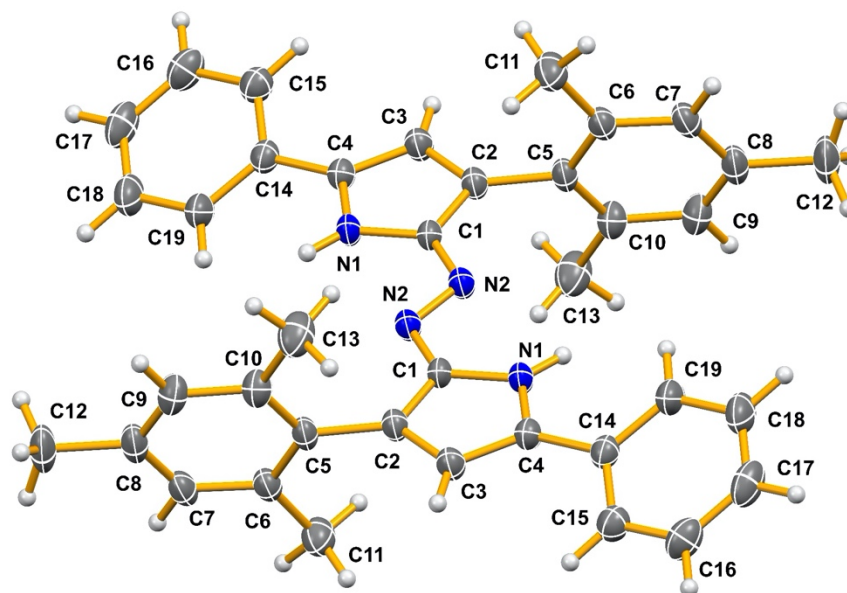


Figure S68: Structure of molecule one in **3** with full labelling. There is an inversion center at the midpoint of the N2-N2' bond so only half of the molecule is needed to describe the independent unit. Thermal ellipsoids have been drawn at the 50% probability level. Hydrogen atoms are included but have not been labelled.

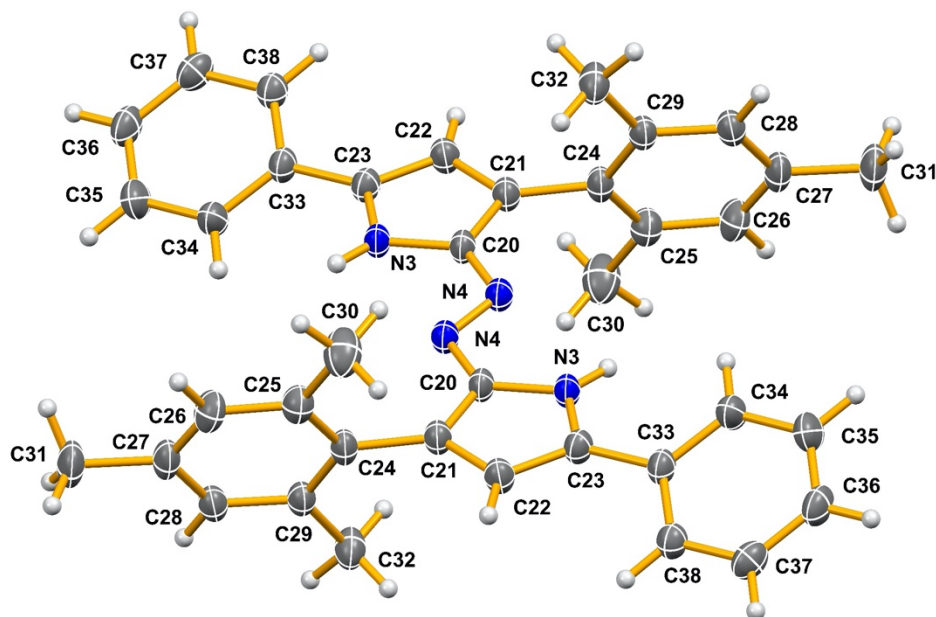


Figure S69: Structure of molecule two in **3** with full labelling. There is an inversion center at the midpoint of the N4-N4' bond so only half of the molecule is needed to describe the independent unit. Thermal ellipsoids have been drawn at the 50% probability level. Hydrogen atoms are included but have not been labelled.

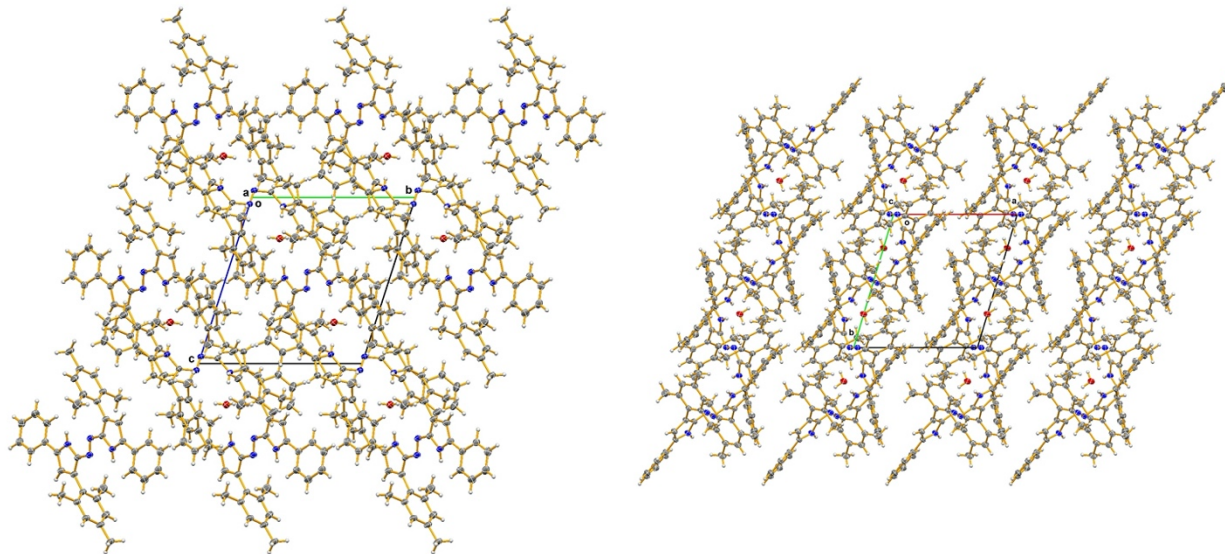


Figure S70: Packing diagrams of compound **3** viewed down the *A* (left) and *C* (right) axes.

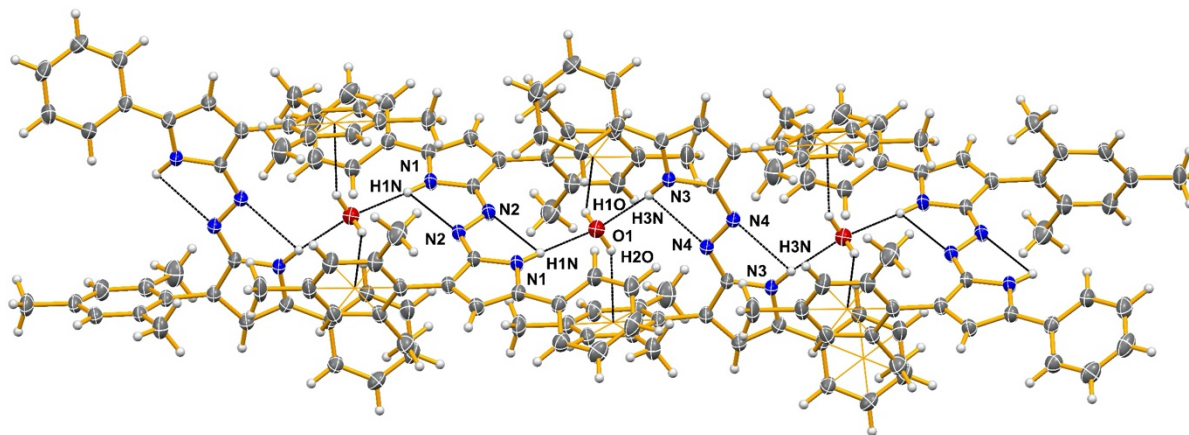


Figure S71: An overall view of the network of hydrogen bonds (dashed lines – less than the sum of the van der Waals radii) in compound **3**. The water molecule forms O-H hydrogen bonds with the acceptors being electron density in aromatic rings of adjacent molecules. Thermal ellipsoids have been drawn with 50% probability. Only selected atoms have been labelled.

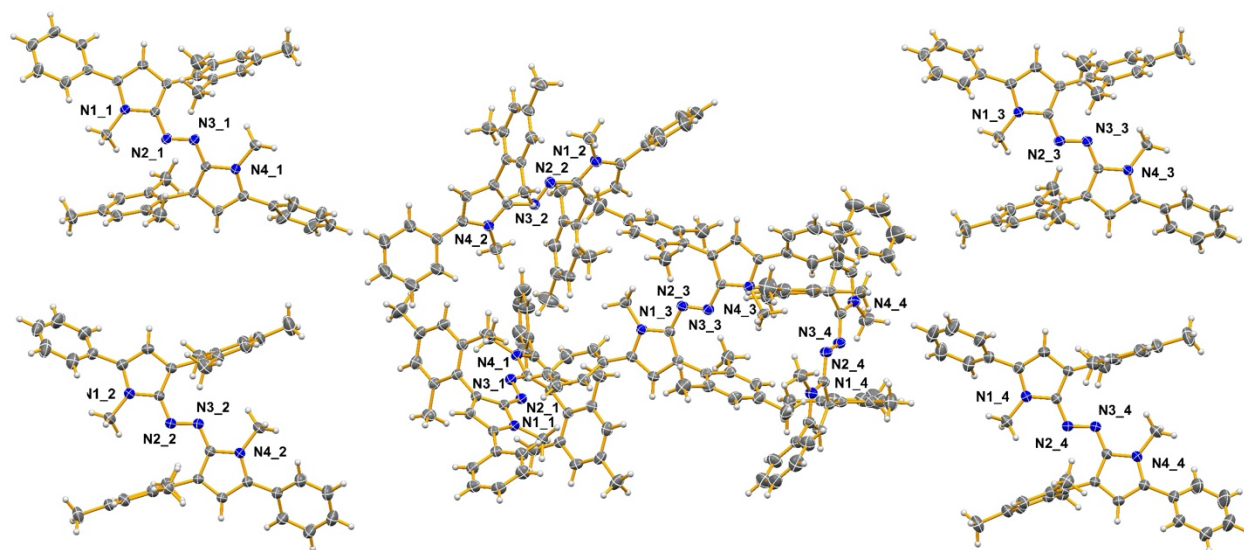


Figure S72: Composite diagram used to describe the structure of compound **5a**. In the center is the arrangement of the four different molecules in the independent unit. On the periphery are each of the four molecules rotated into a similar plane to highlight their similarities and differences. Only the nitrogen atoms in each residue have been labelled. Thermal ellipsoids have been drawn at the 50% probability level. Hydrogen atoms are included but have not been labelled.

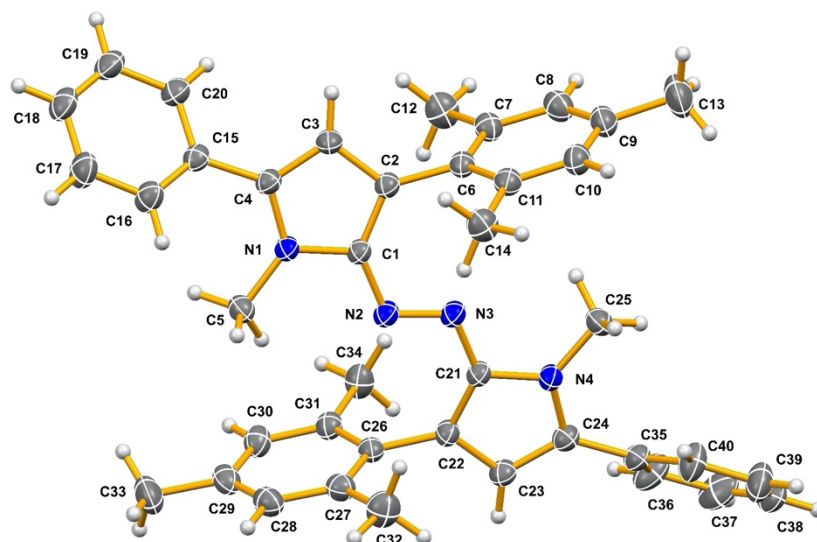


Figure S73: Structure of molecule/residue one in **5a** with full labelling. Because of the large number of atoms in the asymmetric unit (four complete molecules) each molecule was designated as a different residue and given the same numbering scheme. Thermal ellipsoids have been drawn at the 50% probability level. Hydrogen atoms are included but not been labelled.

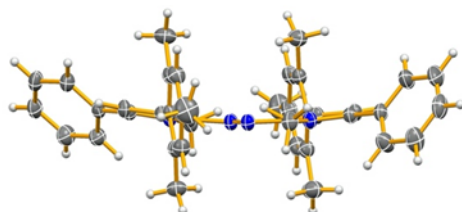


Figure S74: Perpendicular view of molecule/residue 1 in **5a**. Thermal ellipsoids drawn at the 50% probability level. Atoms have not been labelled.

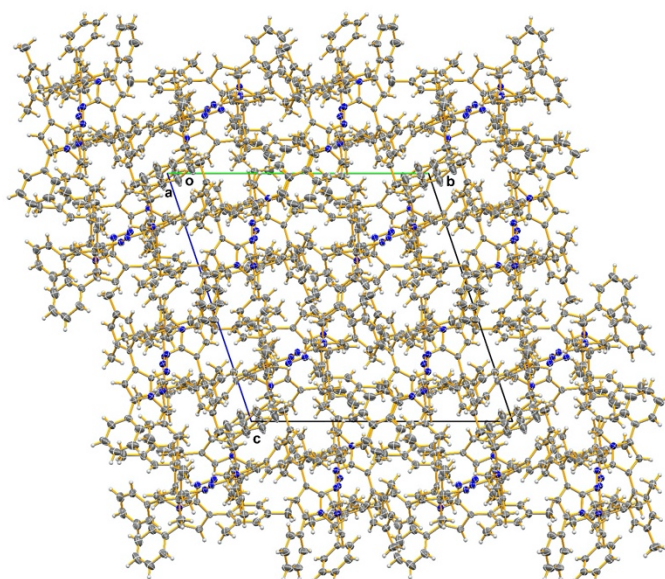


Figure S75: Packing diagrams of compound **5a** viewed down the *A* axis.

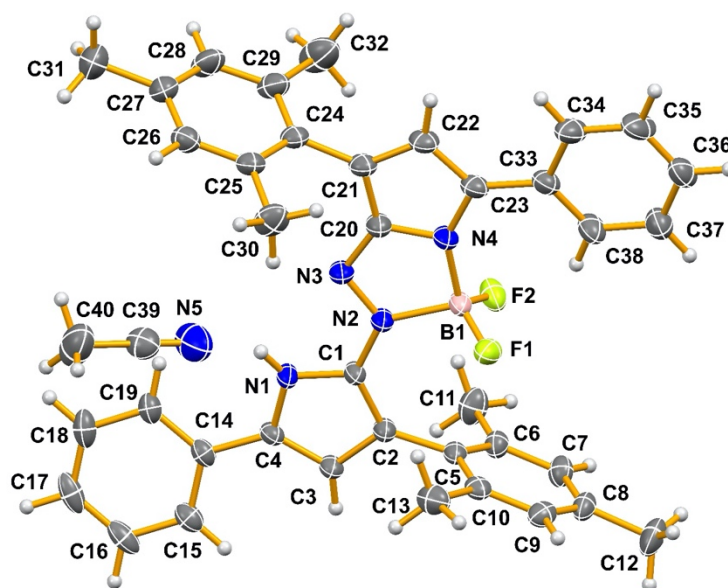


Figure S76: Structure of compound **6** with full labelling, including one molecule of acetonitrile solvent. Thermal ellipsoids have been drawn at the 50% probability level. Hydrogen atoms are included but have not been labelled.

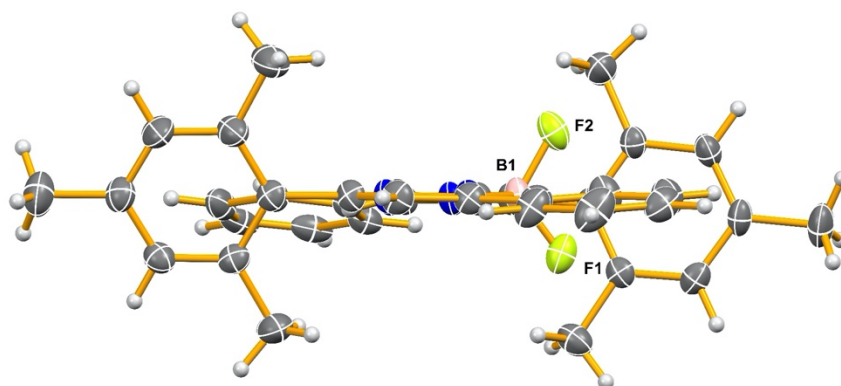


Figure S77: Perpendicular view of compound **6** with the acetonitrile solvent removed. Thermal ellipsoids have been drawn at the 50% probability level. Only selected atoms have been labelled. Hydrogen atoms are included but have not been labelled.

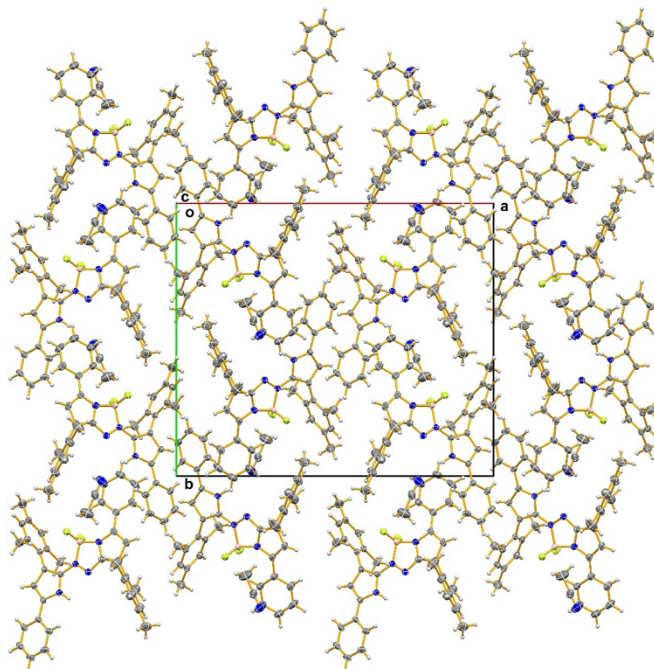


Figure S78: Packing diagrams of compound **6** viewed down the *C* axis.

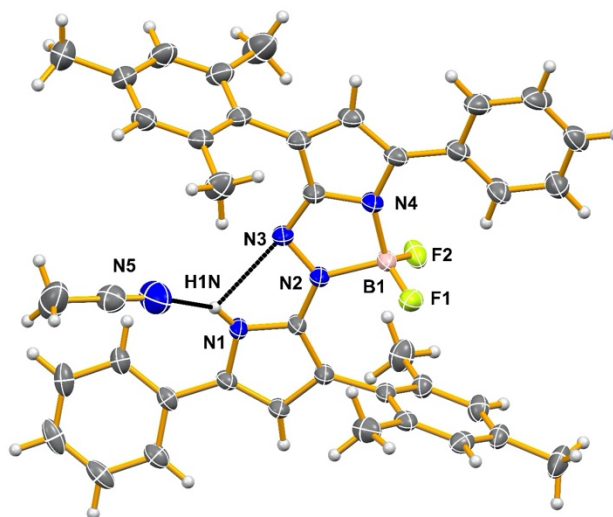


Figure S79: The N-H hydrogen bonds (dashed lines – less than the sum of the van der Waals radii) in compound **6**. Thermal ellipsoids have been drawn with 50% probability. Only selected atoms have been labelled.

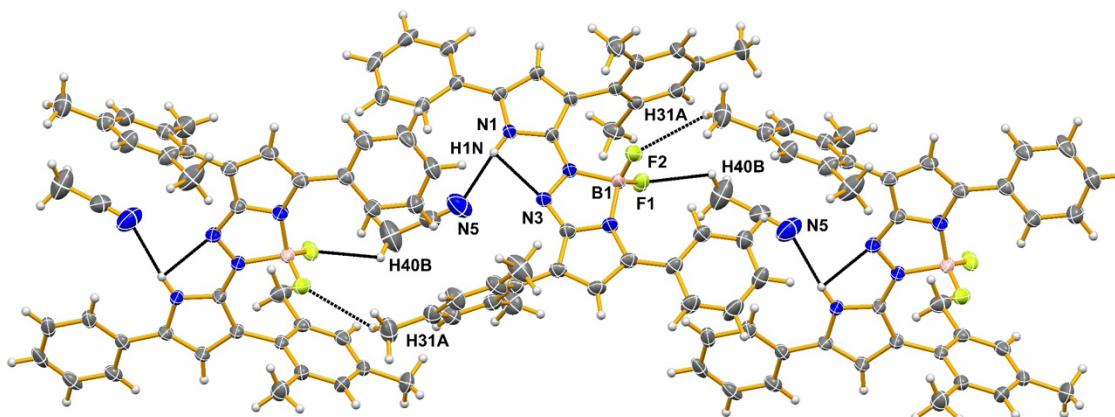


Figure S80: An expanded view of the network of intermolecular interactions (dashed lines – less than the sum of the van der Waals radii) in compound **6**. Both the N-H...N and the C-H...F contacts are included. Thermal ellipsoids have been drawn with 50% probability. Only selected atoms have been labelled.

Discussion of planarity within **3**, **5a** and **6**

BF₂ complex **6**

The central pyrrole-N=N-pyrrole core of the molecule (N1-N4, B1, C1-C4 and C20-C23) encompassing all three rings is essentially planar. The mean deviation of the atoms from this plane is only 0.017 Å. The mesityl rings are also both planar, as expected, with mean deviations of less than 0.006 Å. They lie roughly perpendicular to the central core of the molecule to reduce the steric interactions of the methyl groups on the mesityl ring with the atoms of the central core (84° and 77°). The phenyl rings in this structure are both planar, as expected, and with mean deviations of less than 0.006 Å, as also observed for the mesityl rings. In this structure the phenyl rings lie almost co-planar with central pyrrole-N=N-pyrrole core. The angles between the plane of the central pyrrole-N=N-pyrrole core and the phenyl rings are only 6 and 12°, indicating the phenyl substituents are essentially co-planar with the pyrrole-N=N-pyrrole core. A calculation of the mean plane defined by all of the central core (non-hydrogen) atoms plus all the carbon atoms of the two phenyl rings has a mean deviation of 0.22 Å, a relatively small value considering the number of included atoms. The co-planarity of the phenyl rings with the central core facilitates conjugation through the molecule. It also allows the formation of hydrogen bonding between C38-H38 (phenyl ring 2) and both F1 and F2 of the BF₂ group on one side of the molecule and on the other side H1N can form intramolecular interactions with both H19 (phenyl ring 1) and N3. All of these are likely stabilizing features of the crystal packing adopted.

Dimethyl azo-bispyrrole **5a**

In this compound the nitrogen atom in the 5-membered rings of the central pyrrole-N=N-pyrrole core (N1 and N4 in molecule **1**, for example) have been methylated. By looking at any of the four unique molecules in the asymmetric unit, the presence of these methyl groups evidently causes steric conflicts that disrupt the overall molecular planarity. Molecule **1** has been used for the calculations herein and for comparison purposes in the following discussion. The central pyrrole-N=N-pyrrole core of the molecule (defined by N1-N4, C1-C4 and C21-C24) is planar, with a mean deviation of only 0.13 Å. The two mesityl rings are also planar, as expected, and roughly perpendicular to the central plane, due to steric reasons. The planar phenyl rings (mean deviations

of less than 0.006 Å) make angles of 42° and 28° with the plane of the central pyrrole-N=N-pyrrole core. These angles are not equal and are considerably larger than those observed in compound **6**. A closer investigation of the interactions between the methyl hydrogens and the hydrogen atoms on the phenyl rings showed close intramolecular interactions in all four molecules/residues. In residue 1 H16 of phenyl ring 1 interacts with H5C of the methyl group at a minimum distance of 2.45 Å. In residue 2 the shortest contact is between methyl hydrogen H25 and H40 on the phenyl ring, at 2.30 Å. For residues 3 and 4 the minimum distances are 2.21 Å for H40...H25A and 2.45 Å for H40...H25A, respectively. The steric bulk of the methyl groups, and the need to reduce steric clashes with the phenyl rings, results in the twisting of the phenyl rings out of the planes of the central pyrrole-N=N-pyrrole cores in the four molecules of compound **5a**.

Azo-bispyrrole **3**

There are two unique molecules in the asymmetric unit of this structure. They are joined together by hydrogen bonds formed between one water of hydration and the two molecules of **3**. In this structure, the central pyrrole-N=N-pyrrole cores of both molecules are planar. The core of molecule 1 is defined by N1-N2 and C1-C4 and their symmetry equivalents generated by inversion about a center located at the midpoint of the N2-N2A azo bond. For molecule 2 the equivalent atoms, N3-N4 and C20-C23, are used to define the core, with the inversion center being found at the midpoint of the N4-N4A azo bond. The central cores of the two molecules are planar, with mean deviations of just 0.016 Å and 0.013 Å for molecules 1 and 2, respectively. The mesityl rings and the phenyl rings are each planar, as anticipated, all having mean deviations of less than 0.010 Å. The mesityl rings are, as expected, almost perpendicular to the plane of the central core in each molecule; the angles are 98° in molecule 1 and 77° in molecule 2 (they are equal on each side of the molecule by symmetry). The phenyl rings are also planar, again as of course expected; the mean deviation of the atoms in molecule 1 is 0.005 Å and in molecule 2 it is 0.003 Å. However, in this structure the phenyl rings are not coplanar with the core atoms. Instead, the phenyl planes make angles of 23° with the core in molecule 1 and angles of 22° in molecule 2. These are roughly twice the angles observed in the structure of compound **6**, though less than those observed in the molecules of compound **5a**. In compound **3** there is no methyl group in the core, and thus associated unfavourable steric contacts cannot be the reason that the phenyl groups do not lie coplanar with the central pyrrole-N=N-pyrrole core. Yet, the phenyl groups do indeed twist out of the plane of the central core despite this perhaps seeming at first glance to be less favourable than the extended co-planarity arrangement observed in compound **6**. The key to rationalizing why the lack of co-planarity exists for **3** appears to be the water molecule found in the structure. The oxygen atom of the water molecule lies on the line formed by the intersection of the planes defined by the cores of molecules 1 and 2. This allows a short, symmetrical arrangement of hydrogen bonds to be formed in the structure. First, the hydrogen atoms of the water molecule act as donors in a pair of similar hydrogen bonds involving both molecules 1 and 2. In both cases the hydrogen bond acceptor lies with electron density in the mesityl rings of the molecules, the first being O1-H1O to the mesityl ring of molecule 1 and the second being O1-H2O to electron density of the mesityl ring in molecule 2. The distance to the ring centroid is 2.47 Å in the first interaction and 2.48 Å in the second. In addition, the oxygen atom also acts as the acceptor in a pair of N-H...O hydrogen bonds, again involving both molecule 1, N1-H1N...O1 at 2.11 Å and molecule 2, N3-H3N...O1 at 2.12 Å. Finally, the water molecule also accepts two other hydrogen bonds of distances less than the sum of the van der Waal radii of the interacting atoms. These are C34-H34...O1 (2.61 Å) and C19-H19...O1 (2.65 Å), where both H34 and H19 are hydrogen atoms on the phenyl rings of

molecules 2 and 1, respectively. Neither of these hydrogen bonds approaches linearity (at roughly 140°); however, it is clear that both phenyl rings tilt down towards O1 as a result of these interactions. The formation of these additional C-H...O hydrogen bonds likely provides additional stability in the solid state, and enables reasonable rationalization as to why the phenyl rings are not co-planar with the central pyrrole-N=N-pyrrole core of the molecules in the structure of compound 3.

References

- 1 N. R. Babij, E. O. McCusker, G. T. Whiteker, B. Canturk, N. Choy, L. C. Creemer, C. V. D. Amicis, N. M. Hewlett, P. L. Johnson, J. A. Knobelsdorf, F. Li, B. A. Lorsbach, B. M. Nugent, S. J. Ryan, M. R. Smith and Q. Yang, *Org. Process Res. Dev.*, 2016, **20**, 661–667.
- 2 L. Jiao, Y. Wu, Y. Ding, S. Wang, P. Zhang, C. Yu, Y. Wei, X. Mu and E. Hao, *Chem. Asian J.*, 2014, **9**, 805–810.
- 3 Y. Li, B. O. Patrick and D. Dolphin, *J. Org. Chem.*, 2009, **74**, 5237–5243.
- 4 APEX 4, Bruker AXS Inc., Madison, Wisconsin, USA, 2018.
- 5 SAINT, Bruker AXS Inc., Madison, Wisconsin, USA, 2019.
- 6 SADABS, Bruker AXS Inc., Madison, Wisconsin, USA, 2016.
- 7 G. M. Sheldrick, *Acta Cryst.*, 2015, **A71**, 3–8.
- 8 G. M. Sheldrick, *Acta Cryst.*, 2015, **C71**, 3.
- 9 A. L. Spek, *J. Appl. Cryst.*, 2003, **36**, 7–13.
- 10 C. F. Macrae, I. J. Bruno, J. A. Chisholm, P. R. Edgington, P. McCabe, E. Pidcock, L. Rodriguez-Monge, R. Taylor, J. van de Streek and P. A. Wood, *J. Appl. Cryst.*, 2008, **41**, 466–470.